The EMBO Journal Vol.18 No.9 pp.2593–2609, 1999

The Mex67p-mediated nuclear mRNA export pathway is conserved from yeast to human

Jun Katahira, Katja Straßer, Alexandre Podtelejnikov[1], Matthias Mann[1], Jae U.Jung[2] and Ed Hurt[3]

BZH, Biochemie-Zentrum Heidelberg, Im Neuenheimer Feld 328, D-69120 Heidelberg, Germany, [1]CEBI Odense University, Staermosegaardsvej 16, DK-5230 Odense, Denmark and [2]Department of Microbiology and Molecular Genetics, Harvard Medical School, Boston, MA 02114, USA

[3]Corresponding author
e-mail: cg5@ix.urz.uni-heidelberg.de

Human TAP is an orthologue of the yeast mRNA export factor Mex67p. In mammalian cells, TAP has a preferential intranuclear localization, but can also be detected at the nuclear pores and shuttles between the nucleus and the cytoplasm. TAP directly associates with mRNA *in vivo*, as it can be UV-crosslinked to poly(A)$^+$ RNA in HeLa cells. Both the FG-repeat domain of nucleoporin CAN/Nup214 and a novel human 15 kDa protein (p15) with homology to NTF2 (a nuclear transport factor which associates with RanGDP), directly bind to TAP. When green fluorescent protein (GFP)-tagged TAP and p15 are expressed in yeast, they localize to the nuclear pores. Strikingly, co-expression of human TAP and p15 restores growth of the otherwise lethal *mex67::HIS3/mtr2::HIS3* double knockout strain. Thus, the human TAP–p15 complex can functionally replace the Mex67p–Mtr2p complex in yeast and thus performs a conserved role in nuclear mRNA export.

Keywords: CAN/Nup214/Mex67p/Mtr2p/NTF2/nuclear mRNA export

Introduction

In eukaryotic cells, transport of macromolecules between the nucleus and the cytoplasm occurs through the nuclear pore complexes (NPCs) (Ohno *et al*., 1998). Each NPC, which have a mol. wt of 125 MDa in vertebrates (Reichelt *et al*., 1990) and 66 MDa in yeast (Yang *et al*., 1998), is composed of different subcomplexes containing unique sets of nuclear pore proteins (nucleoporins). By employing biochemical and genetic approaches, physical and genetic interactions of nucleoporins within subcomplexes have been demonstrated. It is likely that the various NPC subcomplexes play different roles in nucleocytoplasmic transport, maintenance of NPC structure and NPC biogenesis (Fabre and Hurt, 1997).

Both small and large karyophilic proteins are imported into the nucleus with the help of a nuclear localization sequence (NLS). An NLS can be a short stretch of basic amino acids (classical NLS or bipartite NLS), or an extended NLS such as the M9 sequence of hnRNP A1, the RGG-box within Npl3p and complex ribosomal NLSs (for review see Mattaj and Englmeier, 1998). These NLSs are recognized either directly by importin/karyopherin β family transport receptors or indirectly via adaptor proteins. The latter is the case for importin/karyopherin α, the receptor for classical and bipartite NLSs (Conti *et al*., 1998), or snurportin, a receptor for snRNPs (Huber *et al*., 1998). Transport substrate–receptor complexes which form in the cytoplasm are translocated through the nuclear pores, most likely by direct contact between FXFG/GLFG/FG-repeat sequences containing nucleoporins and importin/karyopherin β subunits. When the translocated complex meets RanGTP inside the nucleus, the complex dissociates and the bound karyophilic protein is released (for a review see Gorlich, 1998).

Similar to nuclear import, nuclear export of both proteins and RNAs occurs through the nuclear pore complexes and is signal-mediated, and energy- and Ran-dependent (Dahlberg and Lund, 1998). The mechanism of Rev-mediated retroviral mRNA nuclear export is well understood (Ullman *et al*., 1997). Rev binds via its RNA-binding domain to the RRE of unspliced or partially spliced viral mRNA and via its leucine-rich NES to CRM1, also a member of the importin/karyopherin β family transport receptors (Fornerod *et al*., 1997a; Fukuda *et al*., 1997; Ossareh-Nazari *et al*., 1997; Stade *et al*., 1997). Complex formation is cooperative and requires RanGTP. An oligomeric viral pre-mRNA–REV–CRM1–RanGTP complex is then exported through the nuclear pores, again most likely through multiple contacts to nucleoporins with repeat sequences. It is thought that CRM1 makes the association with nuclear pore proteins, since it was found to co-purify with the FG-repeat containing nucleoporin CAN/Nup214 (Fornerod *et al*., 1997b) and exhibits two-hybrid interactions with other FG-repeat containing nucleoporins (Neville *et al*., 1997). Besides the CRM1-dependent export pathway, human and yeast Los1/exportin-t and CAS/Cse1p have been identified as the export receptors for tRNAs and importin α, respectively (Kutay *et al*., 1997, 1998; Arts *et al*., 1998; Hellmuth *et al*., 1998; Kunzler and Hurt, 1998; Solsbacher *et al*., 1998). Based on these observations, the various nuclear export pathways are thought to require a distinct exportin belonging to the β-family (or the combination of several members), which binds cooperatively together with RanGTP to the NES of a given export substrate (Mattaj and Englmeier, 1998).

Concerning mRNA export, several maturation steps such as splicing and modification of pre-mRNA are prerequisite for release of the transport substrate from intranuclear retention sites. It is well known that pre-mRNA becomes associated with many different RNA-binding proteins during or shortly after transcription, forming heterogeneous ribonucleoprotein (hnRNP)

particles (Dreyfuss *et al*., 1993). These hnRNP proteins can be UV-crosslinked to pre-mRNA and thus co-purify with poly(A)$^+$ RNA under denaturing conditions. Interestingly, some hnRNP proteins, such as hnRNP A1, remain associated with mRNAs during transport into the cytoplasm, whereas others, like hnRNP C, dissociate from the mRNA before nuclear exit (Nakielny and Dreyfuss, 1996, 1997). Accordingly, shuttling proteins such as hnRNP A1 are thought to play a direct role in mRNA export. This is in accordance with the finding that hnRNP A1 not only contains a NLS but also a NES as part of the M9 sequence (Michael *et al*., 1995). Thus, in analogy to the Rev/CRM1-mediated viral mRNA export, cellular mRNA-binding proteins may serve as adapters that bridge mRNA and bona fide exportins of the importin/karyopherin β family.

Besides adapter proteins and shuttling transport receptors, NPC components are crucial for mRNA export. Genetic screens and biochemical assays led to the identification of the Nup84p subcomplex in yeast which consists of Nup84p, Nup85p, Nup120p, the C-terminal domain of Nup145p, Sec13p and Seh1p (Siniossoglou *et al*., 1996). The complex is involved in both mRNA export and maintenance of the NPC structure. Using a synthetic lethal (sl) screen using a *nup85* ts allele, a genetic interaction between *MEX67* and *NUP85* was discovered (Segref *et al*., 1997). Mex67p is essential and temperature-sensitive (ts) mutants show rapid and strong intranuclear mRNA accumulation. Furthermore, binding of Mex67p to both poly(A)$^+$ RNA and NPC components was found. Mex67p performs its essential role in mRNA export in conjunction with another factor called Mtr2p (Santos-Rosa *et al*., 1998). In particular, Mex67p requires Mtr2p for stable association with the nuclear pores. Thus, formation of a heterodimeric complex between Mex67p and Mtr2p is essential for mRNA export in yeast.

In mammalian cells, involvement of distinct nucleoporins (e.g. NUP153, CAN/Nup214 and NUP98) in mRNA export has also been implicated (Matunis *et al*., 1992; Bastos *et al*., 1996; Van Deursen *et al*., 1996; Powers *et al*., 1997). However, the precise mechanism of how nucleoporins participate in mRNA exit through the pores is unknown. Interestingly, a human protein called TAP which was first identified in a two-hybrid screen using the herpes virus saimiri tyrosine kinase-interacting protein (TIP) as bait (Yoon *et al*., 1997), shows significant homology to Mex67p and both proteins share a similar domain organization (Segref *et al*., 1997). More recently, TAP was found to be the cellular host factor which specifically recognizes the constitutive transport element (CTE) of D type retroviral mRNAs (Gruter *et al*., 1998). TAP stimulated export of CTE-containing mRNA that was blocked by excess of CTE RNA microinjected in *Xenopus* oocytes. In addition, excess of CTE inhibited export of cellular mRNA, but microinjected recombinant TAP rescued the CTE-mediated inhibition of mRNA export. However, very little is known about the functional properties of the TAP protein, whether it binds to cellular mRNA and how it interacts with components of the mRNA export machinery.

We demonstrate here that TAP binds to poly(A)$^+$ RNA *in vivo* and shuttles between the nucleus and the cytoplasm. By *in vivo* and *in vitro* studies, we found that TAP can bind directly to the FG-repeat domain of nucleoporin CAN/Nup214 and a novel protein with homology to the RanGDP-binding protein nuclear transport factor 2 (NTF2). Since the TAP–p15 complex is functional in yeast, we propose that TAP–p15 functions as an evolutionarily conserved mRNA exporter.

Results

TAP exhibits an intranuclear and NPC localization in mammalian cells

The yeast mRNA export factor Mex67p and a human protein called TAP are homologous (Segref *et al*., 1997). To determine the subcellular localization of human TAP in mammalian cells, polyclonal antibodies were raised against the N- and C-terminal part of TAP in rabbits. On Western blots, these antibodies specifically reacted with bacterially expressed recombinant TAP (data not shown) and authentic TAP derived from HeLa and NIH 3T3 cells (Figure 1A). Whereas in the case of the anti-TAP-C immune serum, no cross-reactivity was seen with a putative *Xenopus* TAP homologue, the anti-TAP-N serum reacted with two bands of higher molecular weight compared with mammalian TAP (Figure 1A). By using both types of anti-TAP antibodies in indirect immunofluorescence, TAP was found to be concentrated inside of the nucleus in mammalian cells, with very little signal in the cytoplasm (Figure 1B). To find out whether a pool of TAP associates with NPCs, HeLa cells were pre-extracted under different conditions before fixation and indirect immunofluorescence (Figure 1C). In particular, when high salt or nuclease was used, a punctate nuclear envelope staining became apparent, which shows that a fraction of TAP exists at the nuclear envelope that is resistant to 0.5 M salt or DNase/RNase treatment, whereas the intranuclear TAP is largely removed by these conditions (Figure 1C). The nuclear rim labeling overlapped with the staining produced by the monoclonal antibody mAb414 that recognizes bona fide NPC antigens (Wente *et al*., 1992). In conclusion, TAP has a predominant intranuclear location in mammalian cells, but a pool of it can also be detected at the nuclear envelope.

TAP shuttles between the nucleus and the cytoplasm

Although TAP localizes predominantly to the nucleoplasm under steady state, it may continuously shuttle between the nucleus and cytoplasm. Since anti-TAP-C antibodies do not crossreact, either on Western blots (Figure 1A) or by indirect immunofluorescence (Figure 2) with a putative *Xenopus* TAP, it was possible to analyze the shuttling of TAP from a mammalian into a *Xenopus* nucleus in a heterokaryon assay by indirect immunofluorescence (Borer *et al*., 1989; Pinol-Roma and Dreyfuss, 1992). The heterokaryons generated here consisted of human HeLa or mouse 3T3 cells fused to *Xenopus* A6 cells. If TAP shuttles, one expects to see transfer of TAP from the mammalian into the *Xenopus* nucleus after heterokaryon formation, in the presence of cycloheximide. A bona fide shuttling (hnRNP A1) and non-shuttling protein (hnRNP C) (Pinol-Roma and Dreyfuss, 1992) served as controls. As can be seen in Figure 2, TAP and hnRNP A1, but not hnRNP C, shuttle between the mammalian and *Xenopus* nucleus. Interestingly, TAP equilibrates between the two types of

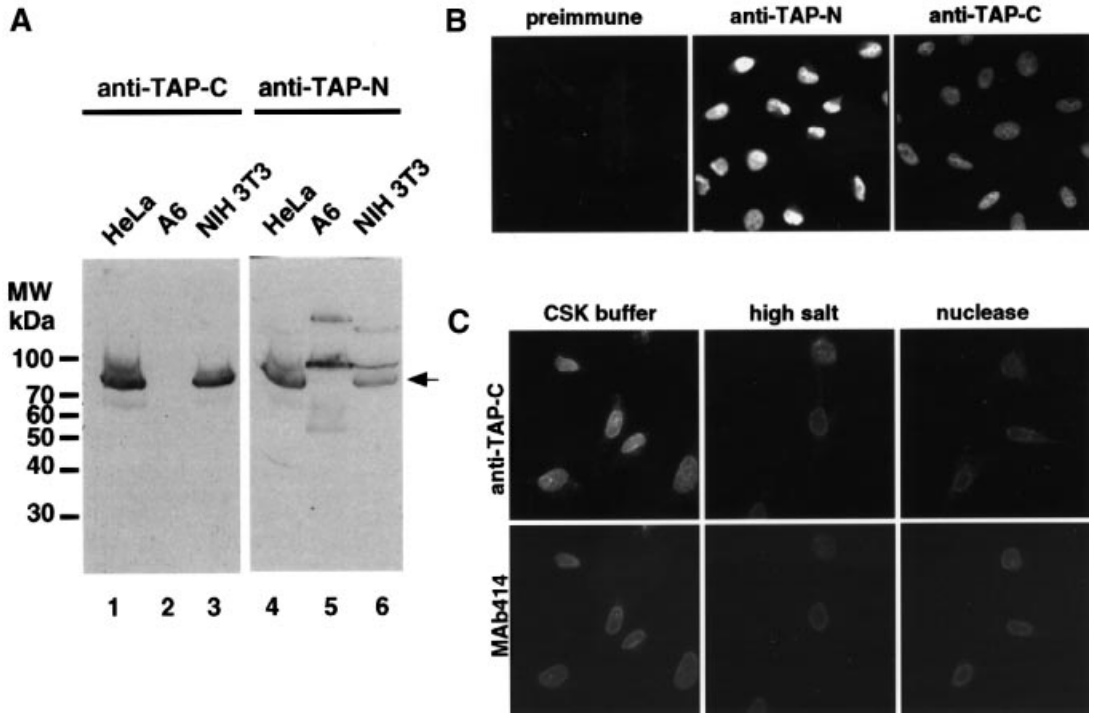

Fig. 1. TAP shows an intranuclear and nuclear envelope location in mammalian cells. (**A**) Western blot analysis to detect TAP in mammalian cells using antibodies against the N-terminal (anti-TAP-N) and C-terminal (anti-TAP-C) domain of TAP. Total cell extracts, which were prepared from the same number (2×10^5) of human HeLa (lanes 1 and 4), *Xenopus* A6 (lanes 2 and 5) and mouse NIH 3T3 (lanes 3 and 6) cells, were separated by SDS–PAGE and transferred onto nitrocellulose membranes. The membranes were incubated with anti-TAP-C (lanes 1–3) and anti-TAP-N antibodies (lanes 4–6) followed by incubation with peroxidase-conjugated goat anti-rabbit IgGs. Bands were visualized by the enhanced chemiluminescence (ECL) method. (**B**) Intracellular localization of TAP in fixed and permeabilized HeLa cells by indirect immunofluorescence using pre-immune, anti-TAP-N and anti-TAP-C antibodies. (**C**) Intracellular localization of TAP in pre-extracted cells using CSK buffer, high salt (0.5 M ammonium sulfate) or DNase/RNase. Cells were double-stained with anti-TAP-C and nucleoporin-specific MAb 414.

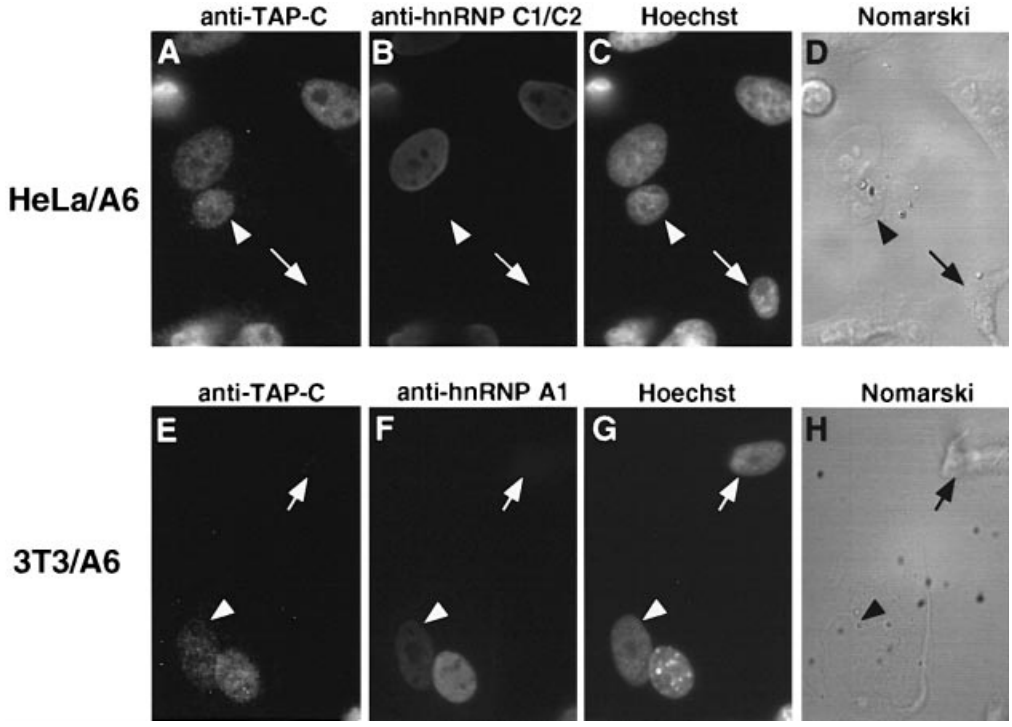

Fig. 2. TAP shuttles between the nucleus and cytoplasm. Heterokaryons were formed between *Xenopus* A6 cells and human HeLa [(**A**)–(**D**)] and mouse NIH 3T3 cells [(**E**)–(**H**)], respectively. Cells were fixed, permeabilized and the distribution of TAP [(A) and (E)], hnRNP A1 (F) and hnRNP C (B) was analyzed by indirect immunofluorescence microscopy using mammalian-specific antibodies. The *Xenopus* nuclei (indicated by arrow heads) were identified by DNA staining with Hoechst 33258 [(C) and (G)]. Note that A6 nuclei in non-fused cells (indicated by arrows) do not exhibit a TAP immunofluorescence signal. Cells were also viewed using Nomarski optics [(D) and (H)].

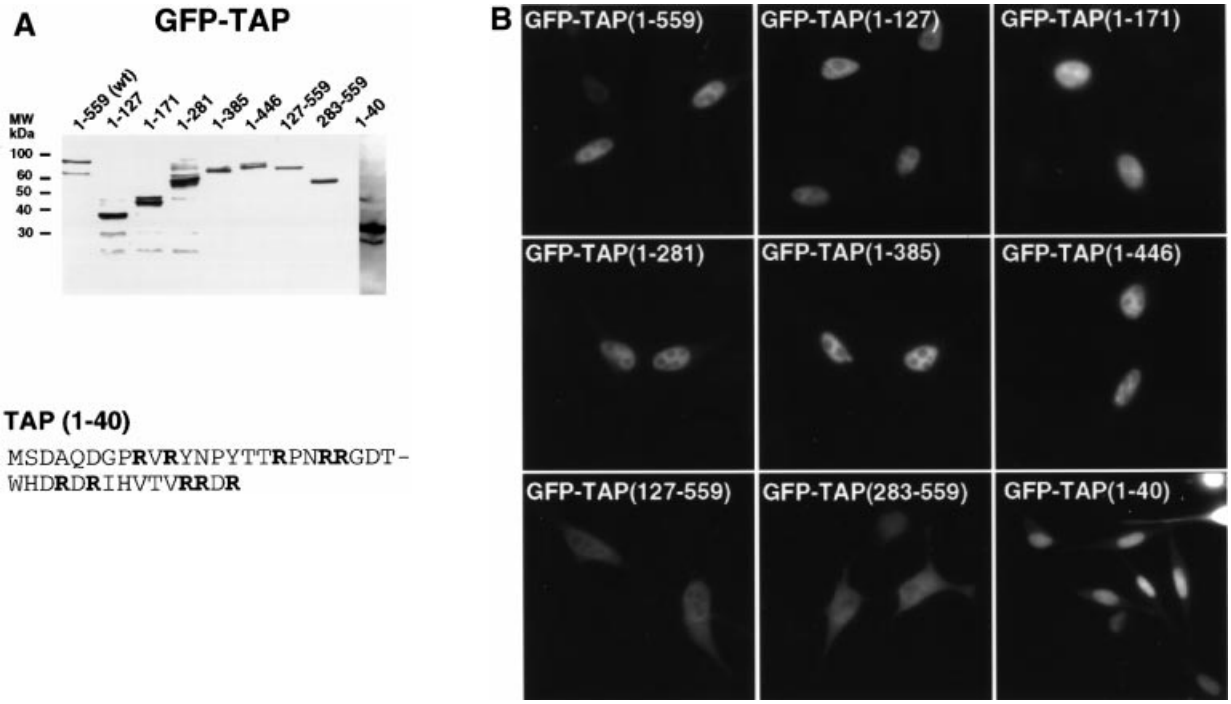

Fig. 3. A NLS within the N-terminal end of TAP. (**A**) Transient expression of full-length GFP–TAP and the various GFP–TAP deletion constructs in HeLa cells was revealed by Western blot analysis using an anti-GFP antibody. Numbers indicate the amino acid length of the corresponding TAP constructs. The primary sequence of the TAP (1–40) is also shown and positively charged amino acids are indicated in bold. (**B**) Subcellular location of GFP–TAP fusion proteins in transfected HeLa cells. Twenty-four hours after transfection, cells were fixed with 4% paraformaldehyde and the subcellular localization of GFP–TAP fusion proteins was determined by fluorescence microscopy.

nuclei (*Xenopus* versus mouse nucleus) with kinetics similar to hnRNP A1 shuttling (Figure 2E, compare with F). Accordingly, TAP shuttles rapidly between the nucleus and the cytoplasm.

TAP contains a nuclear localization signal at its N-terminal end

To determine the NLS within TAP, various TAP deletion constructs were tagged with green fluorescent protein (GFP) and transiently expressed in mammalian cells. All fusion proteins were synthesized according to their expected size with little or no degradation (Figure 3A). Full-length TAP and truncation constructs lacking amino acids from the C-terminal part still accumulated inside the nucleus. GFP–TAP (1–127) was the shortest construct conferring strong nuclear accumulation. On the other hand, a corresponding N-terminal deletion [GFP–TAP (127–559)] exhibits an equal distribution between the nucleus and cytoplasm, with the tendency to accumulate slightly at the nuclear envelope. The NLS within the N-terminal part of TAP could be further restricted to the first 40 amino acids, but in this case a weak cytoplasmic signal also became evident (Figure 3B). This NLS domain within TAP is very basic (pI = 11.5), but it is not clear whether it corresponds to a classical, bipartite or extended NLS (Figure 3A).

TAP can be UV-crosslinked to poly(A)$^+$ RNA in living HeLa cells

If TAP is involved in the nuclear export of cellular mRNA, it may bind directly to its transport substrate. Therefore, we tested whether TAP is bound *in vivo* to poly(A)$^+$ RNA. HeLa cells were UV-irradiated to induce nucleic acid–protein crosslinks and poly(A)$^+$ RNA was purified by oligo(dT) cellulose chromatography under denaturing conditions (Matunis *et al*., 1993). As expected, hnRNP C could be efficiently crosslinked to poly(A)$^+$ RNA (Figure 4A). In contrast, hnRNP A1, known to be less well crosslinked to poly(A)$^+$ RNA (Pinol-Roma *et al*., 1989a), was not significantly detected in the purified poly(A)$^+$ fraction. TAP could be clearly crosslinked to poly(A)$^+$ RNA, but required higher UV-light doses and the efficiency was lower than for hnRNP C. Fibrillarin, which is a nucleolar, snoRNA-associated protein involved in rRNA processing, was not crosslinked to poly(A)$^+$ RNA. This demonstrates that TAP can be directly crosslinked to poly(A)$^+$ RNA *in vivo* and thus associate with mRNA.

In vitro binding of TAP to RNA

Although TAP binds to CTE RNA (Gruter *et al*., 1998) and poly(A)$^+$ RNA, it does not exhibit any known RNA-binding motifs. Therefore, we tested by gel band-shift assay whether TAP, like yeast Mex67p (Santos-Rosa *et al*., 1998), exhibits an *in vitro* RNA-binding activity. Recombinant TAP and various deletion constructs were expressed in *Escherichia coli* as glutathione *S*-transferase (GST)- and histidine-tagged fusion proteins and purified by affinity chromatography. These TAP constructs were then tested for their ability to bind to a ^{32}P-labeled RNA probe, which was synthesized by *in vitro* transcription of the pBluescript SK$^-$ polylinker sequence (Santos-Rosa *et al*., 1998). Whereas histidine-tagged GST alone did not show any affinity to radiolabeled RNA (Figure 4B, lane 1), full-length TAP produced a distinct band shift (Figure 4B, lane 2). This shows that recombinant TAP can bind to RNA *in vitro*. All the C-terminally, but not N-terminally

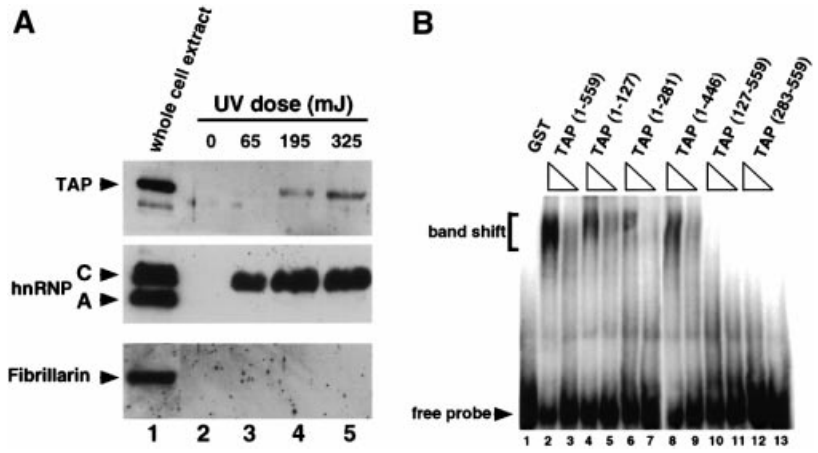

Fig. 4. TAP can be UV-crosslinked to poly(A)$^+$ RNA *in vivo* and binds to RNA *in vitro*. (**A**) Protein–RNA crosslinks were induced by irradiating HeLa cells with UV light and poly(A)$^+$ RNA was purified by oligo(dT) cellulose chromatography. RNase A-treated poly(A)$^+$ RNA (lanes 2–5) and a whole-cell extract (lane 1) were analyzed by Western blotting using anti-TAP-C (upper panel), anti-hnRNP A1 and C1/C2 monoclonal (middle panel) and anti-fibrillarin monoclonal antibodies (lower panel). (**B**) Recombinant TAP can bind to RNA *in vitro*. Full-length TAP and the various deletion constructs, tagged at the N-terminal end with GST followed by six histidines, were partially purified by Ni-affinity chromatography. The eluted proteins were tested for *in vitro* RNA binding using a gel bandshift assay with *in vitro* transcribed and ^{32}P-labeled RNA probe (Santos-Rosa *et al*., 1998). Histidine-tagged GST alone served as negative control. The free RNA probe and the area of the TAP-induced bandshift is indicated as revealed by PAGE and autoradiography. Lane 1, GST-His$_6$ (~4 μg); lanes 2 and 3, ~0.5 and 0.125 μg full-length TAP (1–559); lanes 4 and 5, ~1 and 0.25 μg TAP (1–127); lanes 6 and 7, ~1 and 0.25 μg TAP (1–281); lanes 8 and 9, ~0.5 and 0.125 μg TAP (1–446); lanes 10 and 11, ~1 and 0.25 μg TAP (127–559); lanes 12 and 13, ~1 and 0.25 μg TAP (283–559).

truncated TAP constructs generated RNA band shifts, although less efficiently compared with full-length TAP (Figure 4B, lanes 4–13). Thus, TAP can bind to RNA *in vitro*.

Identification of the human nucleoporin CAN/Nup214 and a novel protein CG1 as TAP-interacting proteins

To examine to which protein(s) TAP binds in human cells, a two-hybrid screen was performed with a human testis cDNA library using full-length TAP as bait. Among the 1.5×10^6 screened colonies, 32 positive clones finally fulfilled the specificity requirements. Of these, 17 contained cDNAs of variable length, but all encoded the C-terminal FG-repeat domain of CAN/Nup214 (Kraemer *et al*., 1994). Clone #291 contained the smallest cDNA insert encoding residues 1805–2090 of CAN/Nup214 (Figure 5A). Further deletions within the C-terminal domain of CAN/Nup214 showed that FG-repeat sequences within the extreme C-terminal end of CAN/Nup214 are essential for the interaction with TAP (Figure 5A, CAN1-4). Recently, an unexpected two-hybrid interaction was reported in which Rip1p (an FG-repeat nucleoporin) interacted with the Rev NES via the bridging protein Xpo1p (Neville *et al*., 1997). We therefore tested whether CRM1/Xpo1p can interact directly with TAP, which may contain a NES. However, no two-hybrid interaction between TAP and Xpo1 was found in the two-hybrid assay (data not shown).

To map the CAN/Nup214-binding domain within TAP, various TAP truncation constructs were tested in the two-hybrid assay. As shown in Figure 5B, all C-terminally truncated, but not N-terminally truncated constructs of TAP were impaired in the interaction with CAN/Nup214. A minimal construct comprising residues 447–559 of TAP still exhibits a HIS$^+$/lacZ$^+$ phenotype in the two-hybrid assay. Thus, part of the middle domain plus the C-terminal domain of TAP (for definition of domain boundaries, see Segref *et al*., 1997) are necessary and sufficient for the interaction with CAN/Nup214.

Interestingly, another two-hybrid cDNA clone was found with TAP as a bait which encodes a sequence highly resembling the FG-domain of CAN/Nup214 or other family members (Figure 5C). The full-length cDNA of this clone is present in the sequence data library as human CG1 (DDBJ/EMBL/GenBank accession No. U97198). Strikingly, hCG1 contains in its non-repetitive C-terminal end a sequence with homology to the corresponding C-domain of yeast Rip1p/Nup42p (Figure 5C). Thus, hCG1, which is not human Rip (Bogerd *et al*., 1995) but appears to be a homologue of yeast Rip1p/Nup42p (Stutz *et al*., 1995), interacts with TAP.

In vitro reconstitution of a TAP–CAN/Nup214 complex

To show that TAP directly binds to CAN/Nup214, GST-tagged CAN4 and CAN3 (see also Figure 5A), as well as GST alone, were expressed in *E.coli* and purified by glutathione–Sepharose chromatography. Partially purified recombinant TAP protein was added to these immobilized GST proteins. After incubation and several washing steps, the bound material was eluted and analyzed by SDS–PAGE and Coomassie staining or Western blotting using anti-TAP antibodies. Clearly, TAP stoichiometrically bound to GST–CAN4, and to a lesser extent to GST–CAN3, but not at all to GST alone (Figure 5D). Thus, the two-hybrid data are consistent with the *in vitro* binding studies which revealed that TAP can interact directly with the FG-repeat domain of CAN/Nup214.

We also addressed the question of whether Mex67p can interact with FG-repeat sequences containing nucleoporins by two-hybrid analysis. Strikingly, full-length Mex67p interacts with the various CAN/Nup214 FG-repeat constructs in a way similar to TAP; a strong HIS$^+$/lacZ$^+$ phenotype was seen with CAN4, less blue color development with CAN3 and no growth and no lacZ activity with

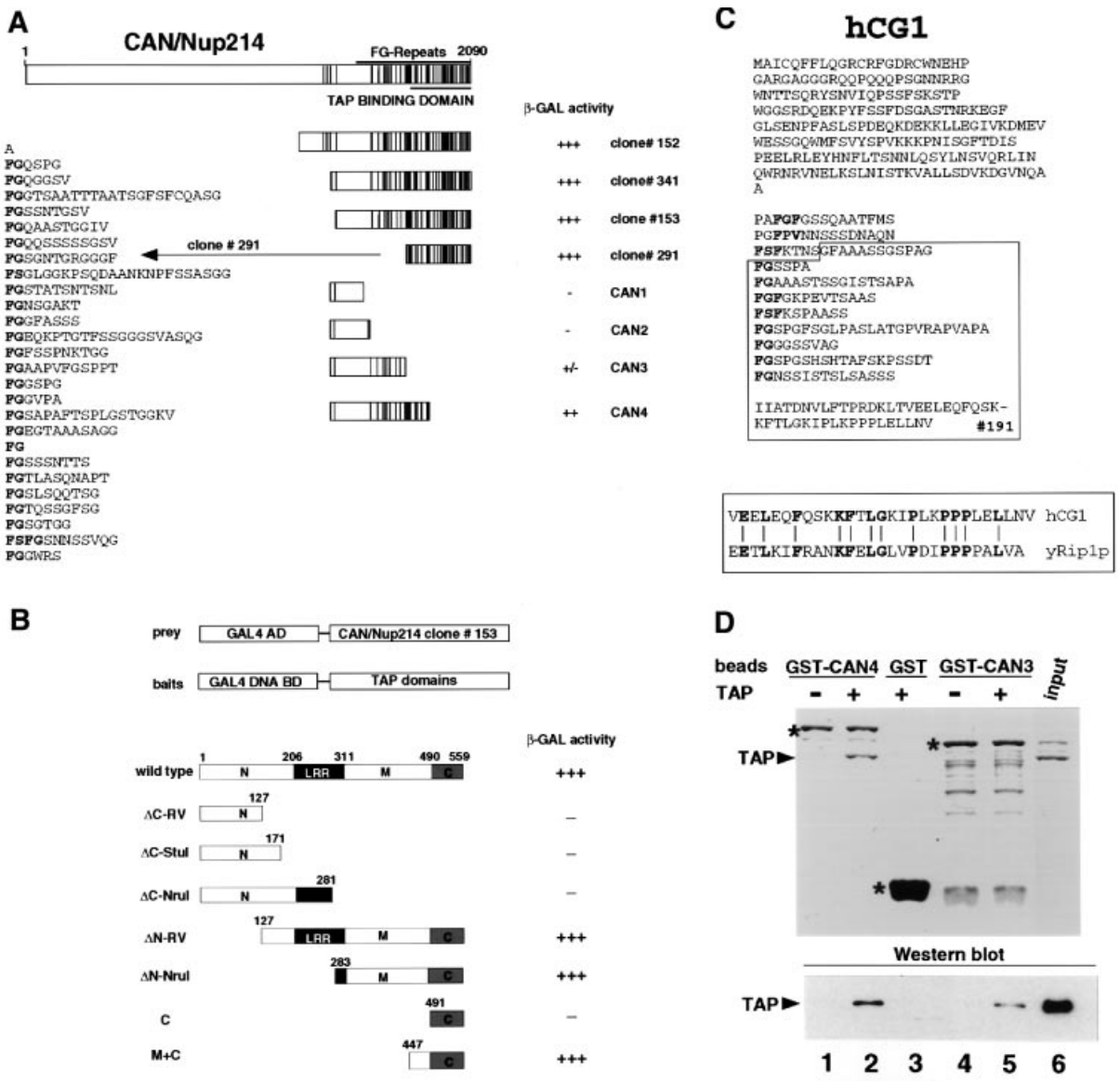
A
CAN/Nup214
1
FG-Repeats
2090
TAP BINDING DOMAIN
β-GAL activity
clone# 152
clone# 341
clone #153
clone# 291
CAN1
CAN2
CAN3
CAN4
clone # 291
A
FGQSPG
FGQGGSV
FGGTSAATTTAATSGFSFCQASG
FGSSNTGSV
FGQAASTGGIV
FGQQSSSSSGSV
FGSGNTGRGGGF
FSGLGGKPSQDAANKNPFSSASGG
FGSTATSNTSNL
FGNSGAKT
FGGFASSS
FGEQKPTGTFSSGGGSVASQG
FGFSSPNKTGG
FGAAPVFGSPPT
FGGSPG
FGGVPA
FGSAPAFTSPLGSTGGKV
FGEGTAAASAGG
FG
FGSSSNTTS
FGTLASQNAPT
FGSLSQQTSG
FGTQSSGFSG
FGSGTGG
FSFGSNNSSVQG
FGGWRS
C
hCG1
MAICQFFLQGRCRFGDRCWNEHP
GARGAGGGRQQPQQQPSGNNRRG
WNTTSQRYSNVIQPSSFSKSTP
WGGSRDQEKPYFSSFDSGASTNRKEGF
GLSENPFASLSPDEQKDEKKLLEGIVKDMEV
WESSGQWMFSVYSPVKKKPNISGFTDIS
PEELRLEYHNFLTSNNLQSYLNSVQRLIN
QWRNRVNELKSLNISTKVALLSDVKDGVNQA
A
PAFGFGSSQAATFMS
PGFPVNNSSSDNAQN
FSFKTNSGFAAASSGSPAG
FGSSPA
FGAAASTSSGISTSAPA
FGFGKPEVTSAAS
FSFKSPAASS
FGSPGFSGLPASLATGPVRAPVAPA
FGGGSSVAG
FGSPGSHSHTAFSKPSSDT
FGNSSISTSLSASSS
IIATDNVLFTPRDKLTVEELEQFQSK-
KFTLGKIPLKPPPLELLNV
#191
VEELEQFQSKKFTLGKIPLKPPPLELLNV hCG1
EETLKIFRANKFELGLVPDIPPPPALVA yRip1p
B
prey
GAL4 AD
CAN/Nup214 clone # 153
baits
GAL4 DNA BD
TAP domains
β-GAL activity
wild type
ΔC-RV
ΔC-StuI
ΔC-NruI
ΔN-RV
ΔN-NruI
C
M+C
N
LRR
M
C
1
206
311
490
559
127
171
281
283
491
447
+++
–
–
–
+++
+++
–
+++
D
beads
GST-CAN4
GST
GST-CAN3
input
TAP
- + + - +
TAP
Western blot
TAP
1 2 3 4 5 6
E
pACTII-CAN3
pACTII-CAN2
pACTII-CAN4
pACTII-CAN1
pAS2-Mex67p bait

CAN2 and CAN1 (Figure 5E). Unfortunately, we could not demonstrate by two-hybrid analysis that Mex67p interacts with Nup159p FG-repeat sequences, since the prey plasmid pACTII containing the FG-repeat domain of Nup159p showed auto-activation (K.Straßer, unpublished results). In conclusion, both Mex67p and TAP interact with FG repeat sequences of CAN/Nup214.

A novel protein homologous to the RanGDP-binding protein NTF2 binds to TAP

Mex67p interacts physically and functionally with Mtr2p and complex formation is essential for mRNA export in yeast (Santos-Rosa *et al*., 1998). To identify a mammalian Mtr2p homologue which binds to TAP, human cells were labeled with [^{35}S]methionine, and TAP was immunoprecipitated under non-denaturing conditions. Strikingly, both anti-TAP-C and anti-TAP-N antibodies immunoprecipitated a 15 kDa protein which was not seen when the pre-immune serum was used (Figure 6A, fluorography). A [^{35}S]methionine-labeled band comigrating with TAP was also precipitated by the pre-immune serum, but this protein is not reactive with anti-TAP-C antibodies on Western blots (Figure 6A, compare fluorography with Western blot). To identify the p15 band, a HeLa nuclear extract (corresponding to 5×10^9 cells) was used as starting material (Figure 6B, lane 1). First, TAP was partially purified from this nuclear extract by MonoS fast performance liquid chromatography (FPLC) (Figure 6B, lane 2), before TAP-containing fractions were subjected to immunoprecipitation using anti-TAP-C antibodies. Under these conditions, TAP was quantitatively immunoprecipitated together with another prominent 15 kDa protein which became visible by SDS–PAGE and silver staining (Figure 6B, lanes 3 and 4). The 70 kDa band was indeed identified as TAP by high sensitivity mass spectrometry (Shevchenko *et al*., 1996a). For the p15 band co-precipitating with TAP, MALDI peptide mapping did not allow its positive identification, indicating that it is a novel protein. Therefore, the peptide mixture was sequenced by nano-electrospray mass spectrometry (Wilm and Mann, 1996; Wilm *et al*., 1996). The peptides were isotopically labeled at the C-terminus by performing the digestion in the presence of ^{18}O water and the resulting peptides were sequenced on a prototype quadrupole time-of-flight instrument (QqTOF). This procedure gives high quality data even at very low protein levels due to the high resolution of the QqTOF instrument and the facile interpretation of the fragmentation spectra of the labeled peptides (Shevchenko *et al*., 1997). Peptide sequence tags, i.e. short amino acid sequences combined with the mass information from the tandem mass spectra (Mann and Wilm, 1994), were assembled from the data. As expected, searching amino acid sequence databases by the peptide sequence tags resulted in no hits, confirming that the protein was novel. The high mass accuracy of the data then allowed straightforward searching of expressed sequence databases (dbEST). Several EST sequences matched the data from the 15 kDa band (Table I). The peptide (Acetyl)-ASVDFKTYVDQACR was matched to an EST sequence as well, indicating that the protein is N-terminally acetylated *in vivo* and pointing to the start of the protein. Accordingly, one of the obtained human ESTs represents the full-length cDNA of p15 (Figure 6C). Surprisingly, the deduced amino acid sequence of the TAP-interacting p15 shows significant homology to NTF2 (a RanGDP-binding protein; BLAST analysis: 26% identity and 43% similarity with three gaps) and a Ras-GAP-binding protein (Figure 6D; also see Discussion). To obtain information about the intracellular localization of p15, antibodies were raised against recombinant and purified p15. As shown by indirect immunofluorescence using affinity-purified anti-p15 antibodies, p15 has a predominant nuclear staining with a clear nucleolar exclusion (Figure 6E). To determine whether a pool of p15 is associated with nuclear pores, HeLa cells were pre-extracted with high salt or nuclease prior to indirect immunofluorescence using affinity-purified anti-p15 antibodies. Similarly to TAP, p15 exhibits a punctate nuclear envelope staining that is resistant to high salt and nuclease treatment (Figure 6E).

To test whether TAP can bind to p15 independently of other factors, histidine-tagged p15 was co-expressed with untagged TAP in *E.coli* and purified by Ni-NTA agarose chromatography. His_6-p15 can associate with TAP directly in *E.coli*, as seen by the efficient co-purification (Figure 7A, lane 1). In contrast, no TAP co-purification was observed when yeast His_6-Ntf2p or the irrelevant protein, His_6-Arc1p, were co-expressed with TAP and purified (Figure 7A, lanes 3 and 4). This shows that TAP, among the many thousand different *E.coli* proteins, can specifically bind to p15. Using the same assembly assay in *E.coli*, it was found that the middle domain of TAP (residues 292–490; see also Figure 5B) represents the p15-binding sequence (Figure 7B). Finally we tested whether p15 interacts with Ran in its GDP-bound form. Therefore, p15

Fig. 5. TAP binds directly to FG-repeat sequences. (**A**) The FG-repeat domain of CAN/Nup214 interacts with TAP in the two-hybrid assay. The CAN/Nup214 amino acid sequence from residue 1–2090 is schematically shown as a box and individual FG-repeat sequences are indicated by vertical lines. β-galactosidase activities were determined for the various two-hybrid clones and the strength of interaction with TAP is indicated by plus and minus signs (+++, very strong; ++, strong; +/–, little; –, no blue color development). The repetitive FG-repeat domain of clone #291 is given as insert. (**B**) The C-terminal domain of TAP interacts with FG-repeats. Two-hybrid interactions between clone #153 (CAN/Nup214 aa 1467–2090) and a series of TAP truncation constructs inserted into pAS2, as revealed by the $HIS^+/lacZ^+$ phenotype. Also shown is the domain organization of TAP and the various truncation constructs. Relative β-galactosidase activities are indicated as described in (A). (**C**) The FG-repeat domain of a novel human protein hCG1 (DDBJ/EMBL/GenBank accession No. U97198) interacts with TAP in the two-hybrid assay. The amino acid sequence of hCG1 is shown and its FG-domain (clone #191) which was found in the two-hybrid screen with TAP is boxed. In the lower part, a sequence comparison between the C-domains of hCG1 and yeast Rip1p/Nup42p is depicted. (**D**) *In vitro* binding of TAP to CAN/Nup214. Bead-immobilized GST (lane 3), GST–CAN3 (aa 1462–1795; lanes 4 and 5) and GST–CAN4 (aa 1462–1909; lanes 1 and 2) were mixed with full-length, untagged TAP (lane 6). Bound proteins (lanes 1–5) were analyzed together with the partially purified TAP fraction (lane 6) by SDS–PAGE and Coomassie staining (upper panel) or Western blotting using anti-TAP-C antibodies (lower panel). The positions of GST alone and GST–CAN fusion proteins are indicated by asterisks, the position of TAP by an arrowhead. Note that for the Western blot, three times more histidine-tagged TAP than in the Coomassie stained gel was loaded. (**E**) Two-hybrid interactions between Mex67p and CAN/Nup214 FG-repeat sequences. The bait plasmid pAS2-MEX67 (full-length) and the various pACTII prey plasmids containing the CAN4, CAN3, CAN2 and CAN1 constructs (see also Figure 5A) were transformed into the yeast strain Y-190. It was first selected on SDC (–leu –trp) plates, before it was streaked onto SDC (–leu –trp –his; + 15 mM 3-AT; + X-Gal) plates. Growth and color development was photographed after 5 days.

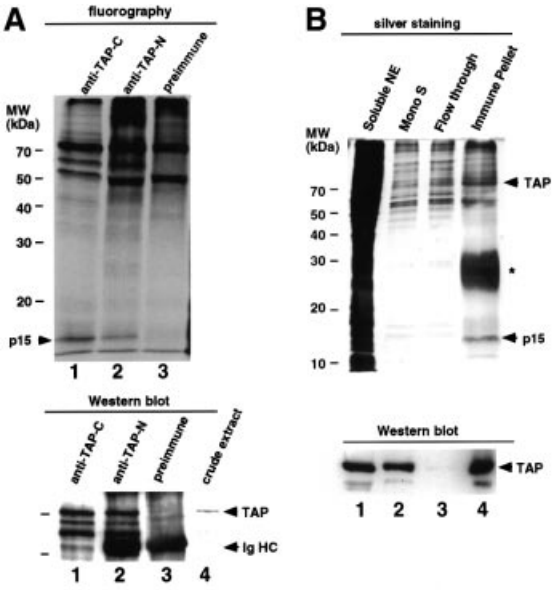

C

p15 sequence

M**ASVDFKTYVDQACRAAEEFVNVYYTTMDKRR**RLLSRLYMGTATLVWNGNAVSGQES
LSEFFEMLPSSEFQISVVDCQPVHDEATPSQTTVLVVICGSVKFEGNKQRDFNQNFI
LTAQASPSNTVWK**IASDCFR**FQDWAS

D

```
                                                 18 19    23       29    33
hNTF2      1 ------MGDKPIWEQIGSSFIQHYYQLFDNDRTQLGAIYIDAS--------
xNTF2      1 ------MAENPIWEQIGASFIQQYYQTFDADRTQLAVIYTDAS--------
yNTF2      1 ------MSLD--FNTLAQNFTQFYYNQFDTDRSQLGNLYRNES--------
GAP-BP     1 -----MVNEKPSPLLVGREFVRQYYTLLNKAPEYLHRFYGRNSSYVHGGV
p15        1 MASVDFKTYVDQACRAAEEFVNVYYTTMDKRPRLLSRLYMGTA--------

                  42                                  66
hNTF2     38 CLTVEGQ-QFQGKAAIVEKLSSLPFQKIQHSITAQDHQPT-PDSC-----
xNTF2     38 CLTVEGQ-QTHGKAAIVEKLSLLPFQKIQHSITSQDHQPT-PDSC-----
yNTF2     36 MLTFETS-QLQGAKDIVEKLVSLPFQKVQHRITTLDAQPASPNGD-----
GAP-BP    46 DASGKPQQAVYGQNDIHHKVLSLNFSECHTKIRHVDAHATLSDG------
p15       44 TLVVNGN-AVSGQESLSEFFEMLPSSEFQ--ISVVDCQPVHDDATPSQTT

                                                          117
hNTF2     81 IISMVVGQLKADED--PIMGFHQMFLKNIN----DAVVCTNDMFRLALH
xNTF2     81 IISMVVGQLKADDD--PIMGFHQVFLKNIQ----DAVVCTNDMFRLALH
yNTF2     80 VLVMITGDLLIDEEQNPQR-FSQVFHKIPDG----NSYYVFNDIFRLNYS
GAP-BP    90 VVVQYMGLLSNSGQ--EFRKFMQTFVLAPEGS-VPNKFYYHNDMFRYEDE
p15       91 VLVVICGTVEFEGN--KQNDFNQNFILTAQASPSNTVWKIASDCFRFQDW

hNTF2    125 NFG-----------
xNTF2    125 NFG-----------
yNTF2    125 A-------------
GAP-BP   137 VFGDSEPELDEESE
p15      139 AS------------
```

E

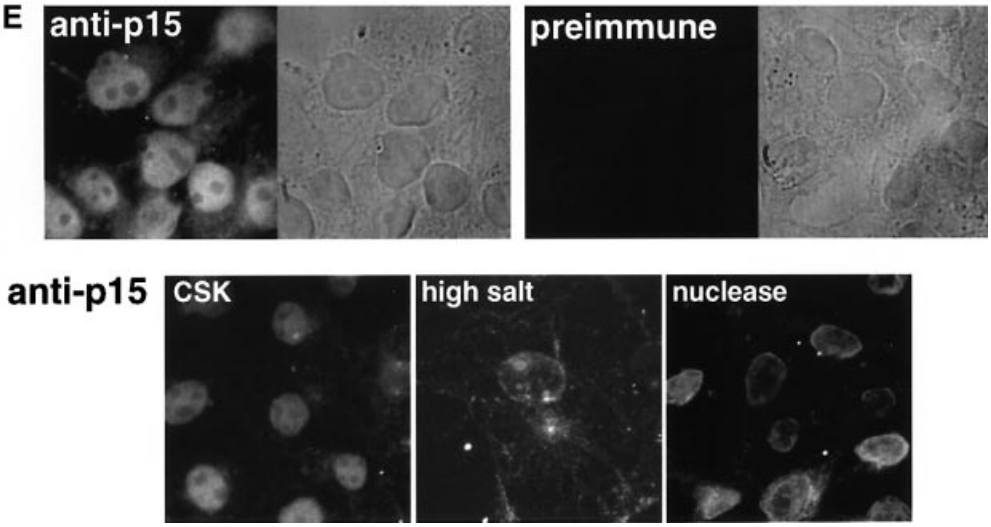

was covalently attached to NHS-activated Sepharose (the coupling efficiency was >80%) and incubated with human Ran (see Materials and methods). However, no binding of p15, neither to RanGDP nor RanGTP was observed (Figure 7C, lanes 5 and 6). Yeast NTF2 served as the control, which was also covalently attached to NHS-activated Sepharose. In this case, yeast NTF2 efficiently bound to RanGDP, but not RanGTP (Figure 7C, lanes 3 and 4). As expected, some NTF2 and GST could be eluted from the Sepharose beads with SDS-sample buffer (Figure 7C). This represents NTF2 or GST molecules, which are part of homodimeric NTF2 or GST complexes, but not covalently crosslinked to the beads. This is not the case for covalently attached p15, which was not eluted from the beads with SDS-sample buffer. This suggests that p15 is a monomer, which is in agreement with another finding that recombinant and purified p15 elutes from a gel filtration Superdex column at a mol. wt of ~14 kDa (data not shown).

The human TAP–p15 complex complements the otherwise lethal mex67–mtr2 null mutant

To test whether human TAP is functional in yeast, it was expressed as a GFP-tagged fusion protein under the control of the *NOP1* promoter and inserted into a high copy plasmid. As seen by fluorescence microscopy, GFP–TAP exhibits a punctate nuclear envelope staining, typical for a NPC location (Figure 8A). To demonstrate that human TAP physically associates with nuclear pores in yeast, GFP–TAP was expressed in nup133$^-$ cells, which have clustered nuclear pores (Doye *et al*., 1994). The GFP–TAP signal co-clustered with NPCs in these mutant cells, indicating that TAP localizes to NPCs under steady-state conditions (Figure 8B). Since the NPC location of Mex67p depends on a functional Mtr2p (Santos-Rosa *et al*., 1998), we examined whether GFP–TAP dissociates from the nuclear pores in *mtr2* mutant cells. Similarly to Mex67p, GFP–TAP also dissociated from the pores and formed cytoplasmic aggregates when mtr2-13 cells were shifted for 15 min to the non-permissive temperature (Figure 8C, 37°C). The steady-state association of GFP–TAP with NPCs thus requires a functional Mtr2p; however, we could not obtain evidence that TAP physically associates with Mtr2p, since no TAP co-enriched with histidine-tagged Mtr2p during affinity purification from *E.coli* (data not shown). In a similar way, p15 tagged with GFP at its N-terminal end was expressed in yeast. GFP–p15 was predominantly seen in the cytoplasm and nucleus, with an increased signal in the nucleus, but no distinct nuclear envelope staining (data not shown). However, when GFP–p15 was co-expressed with TAP in yeast cells, a distinct nuclear envelope location that resembles the GFP–TAP staining was seen in many cells (Figure 8D).

Human TAP alone could not complement the growth defect of either *mex67*$^-$ (Figure 8E) or *mex67-5* thermosensitive cells (data not shown). Therefore, we could not conclude whether TAP fulfills a function in yeast analogous to mammalian cells. Interestingly, in human cells TAP is stably associated with p15, whereas in yeast Mex67p is tightly bound to Mtr2p (Santos-Rosa *et al*., 1998). We therefore tested whether expression of TAP and p15 together can complement yeast mex67 and mtr2 mutants. Surprisingly, co-expression of human TAP and human p15 enabled mtr2 and mex67 thermosensitive mutants to grow at the restrictive temperature (data not shown). In contrast, TAP or p15 alone were not able to restore growth at 37°C in these strains. This prompted us to test whether the TAP–p15 complex is able to complement the lethal phenotype of strains with a complete knockout of the *MEX67* or *MTR2* genes. If TAP alone or p15 alone were expressed, they were not able to restore growth of the mex67 or mtr2 null mutant (Figure 8E). Strikingly, co-expression of TAP and p15 in either mtr2$^-$ or mex67$^-$ cells enabled them to grow at 23°C (Figure 8E). The

Table I. Identification of the p15 band by mass spectrometry

Peptide mol. wt (Da)	Sequence determined by MS/MS	DDBJ/EMBL/ GenBank accession No.
1935.75	AAEEFVNVYYTTMDKR	W99147
1951.86	AAEEFVNVYYTTMoxDKR	AA050591
2091.90	AAEEFVNVYYTTMDKRR	W89287
2107.95	AAEEFVNVYYTTMoxDKRR	AA571979
		AA717005
		AA790461
881.40	IASDCacrFR	W99147
867.38	IASDC*FR	AA050591
		W89287
		AA571979
		AA717005
		AA790461
1700.76	N-terminal peptide	
	(Acetyl)ASVDFKTYVDQAC*R	gi|792242
		gi|1429129
		gi|1530281
		gi|1542259
		gi|2257022
		gi|2346908
		gi|2850581

Results of EST database searches with a sequence information obtained by tandem mass spectrometry. C*, Cys carbamidomethyl; Mox, oxidized Met; Cacr, Cys arcylamide.

Fig. 6. p15 is a novel TAP-interacting protein with homology to NTF2. (**A**) Immunoprecipitation of TAP from radiolabeled HeLa cells using anti-TAP-C (lane 1), anti-TAP-N antibodies (lane 2), and the pre-immune serum (lane 3). Immune pellets were analyzed by SDS–14% PAGE and bands were visualized by fluorography (upper panel) or Western blotting using anti-TAP-C antibodies (lower panel). A non-labeled whole-cell HeLa extract was also loaded (lane 4). The p15, TAP and Ig heavy chain (Ig HC) bands are indicated. (**B**) Purification of p15. A HeLa nuclear extract (lane 1), the TAP-containing fraction from the MonoS column (lane 2), the flow through (lane 3) and immunoprecipitated TAP (lane 4) were analyzed by SDS–14% PAGE and silver staining (upper panel) or Western blotting using anti-TAP-C antibodies (lower panel). Immunoglobulin light chain is marked by an asterisk. (**C**) Amino acid sequence of the human p15 protein. The peptides obtained by mass spectrometry analysis and sequencing are shown in bold. (**D**) Multiple sequence alignment of p15 with NTF2 proteins from human, *Xenopus* and yeast and a RasGAP-binding protein (GAP-BP). (**E**) Intracellular localization of p15 in HeLa cells. Cells were fixed and permeabilized with 0.2% Triton X-100 (upper panel), or pre-extracted with CSK, high salt or nuclease buffer (lower panel) before fixation. Indirect immunofluorescence was then perfomed using affinity-purified anti-p15 antibodies followed by incubating with Alexa 488-labeled anti-rabbit IgG (Molecular Probes Inc., Eugene, OR) as described in the Materials and methods.

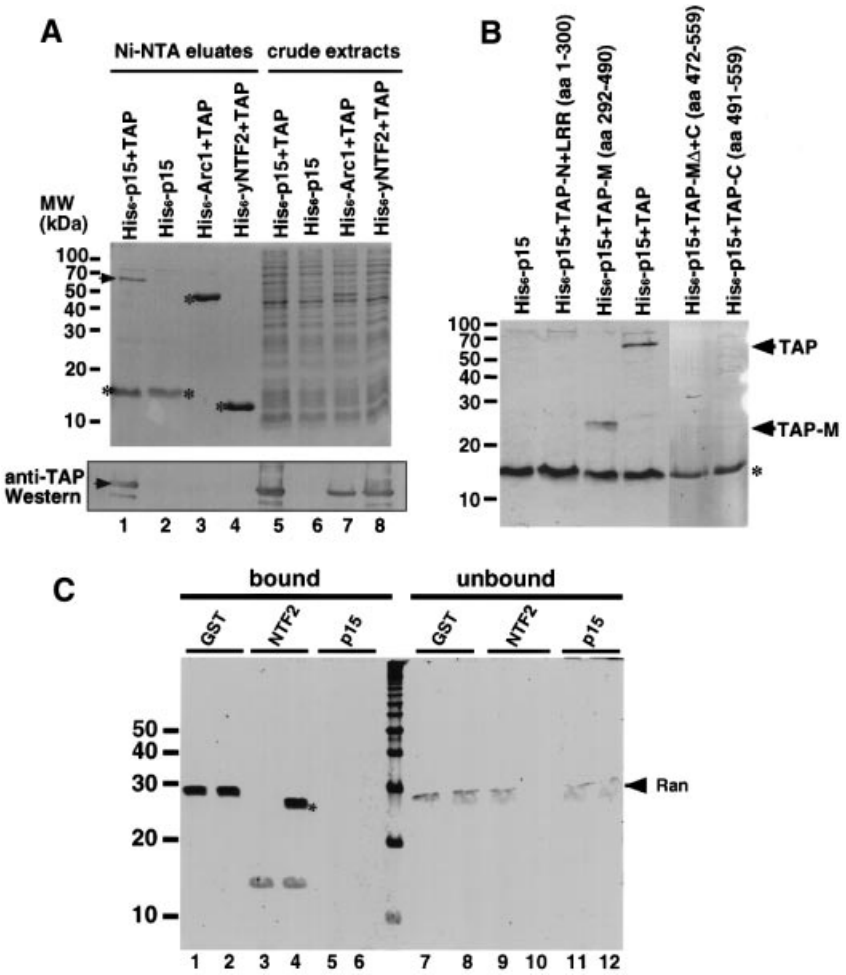

Fig. 7. *In vitro* complex formation between p15 and TAP. (**A**) *E.coli* BL21 cells harboring pET9d-TAP (untagged TAP; lanes 1, 3–5, 7–8) or the empty vector pET9d (lanes 2 and 6) together with pET8c-His_6-p15 (lanes 1 and 5), pET8c-His_6-Arc1 (lanes 3 and 7) or pET8c-His_6-yNTF2 (lanes 4 and 8) were induced and His_6-tagged fusion proteins were purified by Ni-NTA chromatography. Proteins bound to beads were eluted with 200 mM imidazole. Eluates (lanes 1–4) and corresponding whole-cell extracts (lanes 5–8) were subjected to SDS–14% PAGE, followed by Coomassie staining (upper panel) or Western blotting using anti-TAP-C antibodies (lower panel). The positions of histidine-tagged proteins and untagged full-length TAP are indicated by asterisks and arrow heads, respectively. (**B**) Identification of the p15-binding domain within TAP. *Escherichia coli* cells harboring pET8c-His_6-p15 plus pET9d, pET9d-TAP, pET9d-TAP-M (aa 292–490), pET9d-TAP-N+LRR (aa 1–300), pET9d-TAP-MΔ-C (aa 472–559) or pET9d-TAP-C (aa 491–559) were subjected to the same binding assay described in (A). The positions of histidine-tagged p15 and untagged TAP are indicated by asterisks and arrow heads, respectively. (**C**) Comparison of Ran-binding abilities of p15 and yNTF2. Purified GST (lanes 1, 2, 7, 8), histidine-tagged yeast NTF2 (lanes 3, 4, 9, 10), and p15 (lanes 5, 6, 11, 12) were covalently attached to NHS-activated Sepharose (Pharmacia, Freiburg, Germany) resin. The beads were incubated with 1 μg of Ran in its GTP-bound (lanes 1, 3, 5, 7, 9, 11) or GDP-bound (lanes 2, 4, 6, 8, 10, 12) form. After incubating at 4°C for 1 h, the beads were washed and bound material was eluted by boiling in SDS–PAGE sample buffer. A Coomassie Blue stained SDS–polyacrylamide gel of the bound (lanes 1–6; 25% of total) and unbound (lanes 7–12; 7.5% of total) fractions is shown.

human TAP–p15 complex finally restored growth of the otherwise non-viable mex67$^-$–mtr2$^-$ double mutant (Figure 8F). However, complemention was only partial since cells grow more slowly at 23 or 30°C as compared with wild-type cells, and are thermosensitive for growth at 37°C (Figure 8F). This shows that the human TAP–p15 complex is functional in yeast, but cannot fully replace its homologous yeast counterpart. To verify in an independent way that mex67$^-$ and mtr2$^-$ cells complemented by TAP–p15 do not express Mex67p and Mtr2p, Western blot analyis of whole-cell extracts was performed using antibodies against Mex67p, Mtr2p and human TAP. This revealed protein expression patterns as predicted from the genetic work. The single disrupted strains *mex67::HIS3* and *mtr2::HIS3* lacked Mex67p and Mtr2p, respectively, and the double disrupted mutant *mex67::HIS3*/*mtr2::HIS3* lacked both Mex67p and Mtr2p (Figure 8G). However, all these strains express human TAP (Figure 8G). Taken together, this work demonstrated that TAP requires its small binding partner p15 for complementation of either the mtr2 or mex67 single disruption mutants. Since TAP–p15 also restores growth of the mex67–mtr2 double knockout strain, the TAP–p15 complex is functionally homologous to the yeast Mex67–Mtr2p complex (see Discussion).

Discussion

Previously, we suggested that human TAP is the putative homologue of the yeast mRNA export factor Mex67p. We now present experimental evidence that TAP has characteristics of a nuclear mRNA export factor in mam-

malian cells. First, we show that TAP shuttles between the nucleus and the cytoplasm. Secondly, TAP directly binds *in vivo* to poly(A)$^+$ RNA. Thirdly, TAP directly interacts with FG-repeat sequences of the nucleoporin CAN/Nup214 and accordingly can associate with nuclear pores. Fourthly, TAP tightly interacts *in vivo* and *in vitro* with a novel protein that is related to NTF2, a RanGDP-binding protein. Together with the previous findings that TAP is involved in viral CTE-dependent RNA export and recombinant TAP can overcome an mRNA export block caused by saturating amounts of CTE RNA (Gruter *et al*., 1998), our data suggest that TAP is a general nuclear export factor for cellular mRNA in vertebrate cells.

Is TAP a novel type of mRNA export factor?

As known from the yeast system, many nucleoporins are required for nuclear mRNA export (Fabre and Hurt, 1997). Several mammalian nuclear pore proteins such as CAN/Nup214, Nup98 and Nup153 were also implicated in mRNA export (Bastos *et al*., 1996; Van Deursen *et al*., 1996; Powers *et al*., 1997). It is assumed that importin/karyopherin β family receptors bind directly to nucleoporins with FXFG, GLFG or FG repeat sequences, thereby facilitating translocation through the pore channel (Rexach and Blobel, 1995). Accordingly, a putative β-family exportin could bind in the presence of RanGTP to both mRNA (either directly or indirectly via adapter proteins) and FG-repeat nucleoporins. In yeast, a mutant mapping in the exportin CRM1/Xpo1p is not only impaired in leucine-rich NES-mediated nuclear protein export, but also in mRNA export (Stade *et al*., 1997). However, microinjection of Rev NES peptides in *Xenopus* did not impair mRNA export, although snRNA and 5S rRNA export was inhibited (Fischer *et al*., 1995). Accordingly, importin/karyopherin β-type transport receptors could play a role in mRNA export, but it is still under debate whether they are directly involved in this process (for further discussion see Santos-Rosa *et al*., 1998; Stutz and Rosbash, 1998).

One of our key results is that TAP/hMex67, which is not an importin β family member, can make direct contact to the FG-repeat domain of CAN/Nup214 and possibly other nucleoporins. Indeed, an uncharacterized human protein hCG1, which is related to yeast Rip1p/Nup42p, was found to interact with TAP via its FG-repeat domain. Since different nucleoporins with repeat sequences line the entire pore channel, from the nuclear basket to the cytoplasmic pore filaments, TAP with bound RNA could pass though nuclear pores via multiple contacts to FG-repeat nucleoporins. Alternatively, the observed direct contact between TAP and CAN/Nup214 may be used during re-import of the shuttling TAP protein. Although CAN/Nup214 would be strategically located at the cytoplasmic filaments (Kraemer *et al*., 1994; Boer *et al*., 1997), we find this scenario less likely, since TAP contains a basic NLS in its N-terminal domain suggesting that it uses an importin β family transport receptor for its nuclear uptake.

It is conceivable that direct contact between TAP and CAN/Nup214 is one of the last steps during mRNA export, consistent with the finding that CAN/Nup214 plays a role in mRNA export (Van Deursen *et al*., 1996). Interestingly, CAN/Nup214 appears to be the homologue of yeast Nup159p (Belgareh *et al*., 1998; Hurwitz *et al*., 1998; S.Bailer and E.Hurt, unpublished results). Nup159p like CAN/Nup214 is located at the cytoplasmic side of the NPC (Kraemer *et al*., 1995) and is involved in mRNA export, but not protein import (Del priore *et al*., 1997). Interestingly, Mtr2p and Mex67p interact physically and genetically with the Nup84p complex (Santos-Rosa *et al*., 1998) which is also located at the cytoplasmic face of the NPC (B.Fahrenkrog and N.Pante, personal communication). Thus, the release of mRNPs from cytoplasmic NPC structures both in yeast and higher eukaryotes could be the crucial step in terminating mRNA export (see discussion in Santos-Rosa *et al*., 1998).

Possible functions of TAP-associated p15

In all cases that have been tested, the small GTPase Ran and its activity-modulating effectors RanGAP (RNA1) and RanGEF (RCC1) play an important role in mRNA export (for a review see Dahlberg and Lund, 1998). Surprisingly, we found p15, an NTF2-like protein, associated with TAP. Accordingly, p15 may associate with Ran. However, no binding of recombinant p15 or reconstituted p15–TAP to either RanGTP or RanGDP could be observed. Although these negative data do not exclude the possibility that p15 binds transiently to Ran *in vivo*, it is possible that p15 interacts with other targets belonging to the RasGTPase superfamily. The crystal structure of NTF2 has been solved (Bullock *et al*., 1996) and its interaction with RanGDP is known at the atomic level (Stewart *et al*., 1998). Accordingly, the hydrophobic cavity of NTF2 which is made up of several conserved hydrophobic residues (e.g. Y-18 and Y-19; note that these tyrosines are conserved in p15; see Figure 6D) binds an exposed aromatic residue (Phe72) within RanGDP. One can speculate that p15 also contains this hydrophobic pocket and thus could interact with RanGDP or another Ran-like GTPase.

It is interesting to note that a cellular protein called E1B-AP5 (which binds to the Adenovirus RNA transport regulator E1B 55 kDa) and hnRNP U (which is homologous to E1B-AP5), contain a putative GTP-binding domain with homology to Ran and other GTPases (Gabler *et al*., 1998). It is thus conceivable that this type of RNA-binding protein, given that they possess a GTPase activity, could act as a molecular switch to release mRNPs from their site of synthesis and assembly. If TAP can bind via p15 to such a putative GTPase, release of the mRNP from intranuclear sites could be coupled with loading of the export factors (e.g. TAP) onto the transport cargo. Alternatively, p15 may bind to RanGDP in the cytoplasm which could be a trigger for release of TAP from the nuclear pores and/or disassembly of the mRNP/TAP–p15 complex. Identification of a putative target GTPase(s) of p15 should clarify which of these models is correct.

Finally, p15 protein may contribute to NPC targeting of TAP and passage through the pore channel. This possibility is proposed on the basis that (i) NTF2 can directly bind to FXFG-repeat containing nucleoporins p62 and Nsp1p (Percipalle *et al*., 1997), and (ii) NTF2 was identified as a nuclear import factor of RanGDP (Ribbeck *et al*., 1998). Similarly to TAP, a fraction of p15 was localized to the nuclear pores as revealed by indirect immunofluorescence. Accordingly, p15 may also bind to repeat sequence-containing nucleoporins, thereby facilitating nuclear export of TAP and its bound transport substrate.

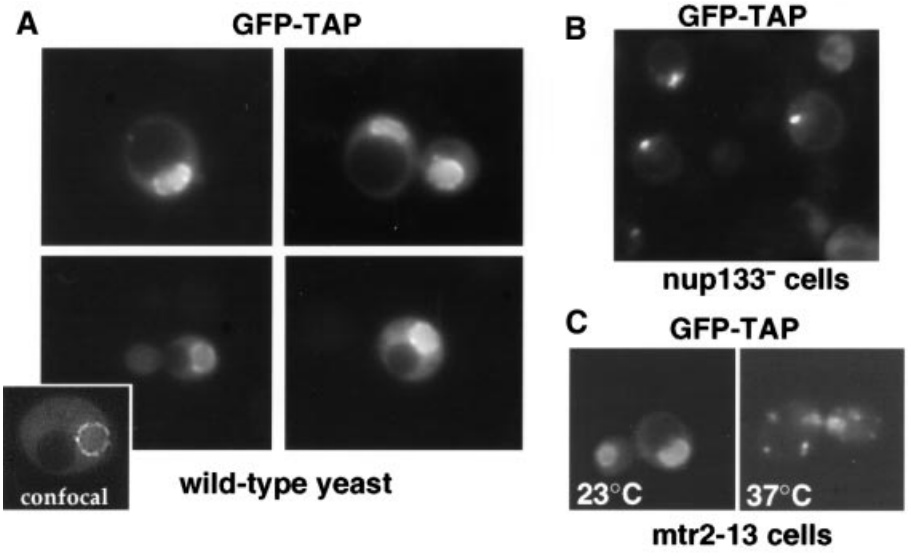
A
GFP-TAP
confocal
wild-type yeast
B
GFP-TAP
nup133⁻ cells
C
GFP-TAP
23°C
37°C
mtr2-13 cells

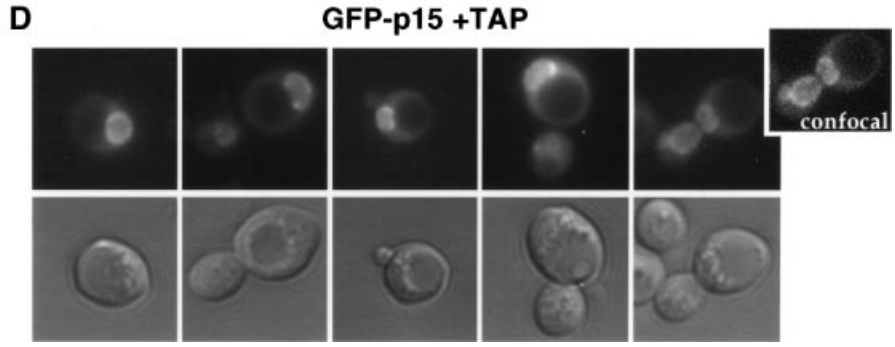
D
GFP-p15 +TAP
confocal

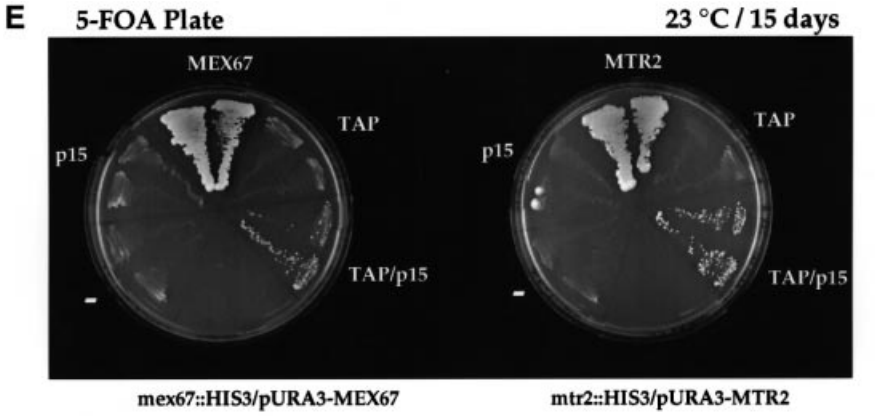
E
5-FOA Plate
23 °C / 15 days
MEX67
TAP
p15
TAP/p15
-
MTR2
TAP
p15
TAP/p15
-
mex67::HIS3/pURA3-MEX67
mtr2::HIS3/pURA3-MTR2

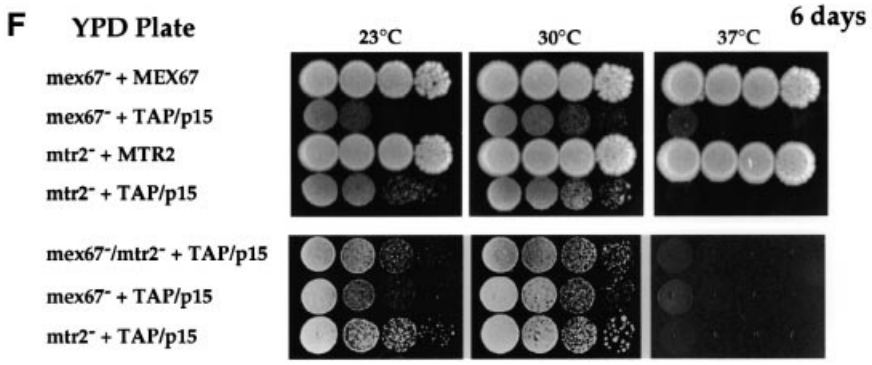
F
YPD Plate
6 days
23°C
30°C
37°C
mex67⁻ + MEX67
mex67⁻ + TAP/p15
mtr2⁻ + MTR2
mtr2⁻ + TAP/p15
mex67⁻/mtr2⁻ + TAP/p15
mex67⁻ + TAP/p15
mtr2⁻ + TAP/p15

Whether this involves multiple contacts to the same FG-repeat sequence-containing nucleoporins to which TAP also binds, or interactions with other nucleoporins to which TAP cannot directly bind, remains to be shown.

In this context, it is also worth mentioning that human p15 is functionally similar to yeast Mtr2p (see below). Mtr2p was shown to interact with the Nup84p complex in yeast and is required for the binding of Mex67p to the nuclear pores under steady-state conditions (Santos-Rosa *et al*., 1998).

The human TAP–p15 complex is functionally homologous to the yeast Mex67p–Mtr2p complex

Apparently, no p15 homologue except NTF2 exists in yeast (E.Hurt, unpublished data). Thus, the function of p15 may have evolved later in evolution. It is also possible that the p15 function is fulfilled by a different protein in *Saccharomyces cerevisiae*. Interestingly, Mtr2p forms a complex with Mex67p in yeast (Santos-Rosa *et al*., 1998). Mtr2p and p15 are small proteins which bind to the middle domain of Mex67p (E.Hurt, unpublished data) and TAP (this work), respectively. It was therefore tempting to test whether Mtr2p and p15 perform a similar function, despite the fact that both proteins do not exhibit significant sequence similarity. To our surprise, the TAP–p15 complex is functional in yeast and not only associates with nuclear pores, but also complements the *mex67::HIS3* and *mtr2p::HIS3* disruption mutants. In contrast, TAP or p15 alone do not exhibit such a complementing activity. Since TAP and p15 are also able to restore growth of the otherwise non-viable *mex67:HIS3*/*mtr2::HIS3* double knockout strain, the human TAP–p15 complex can provide the essential functions exerted by the yeast Mex67p–Mtr2p complex. However, the TAP–p15 complex cannot fully substitute for the Mex67p–Mtr2p complex, since the complemented strain grows more slowly at physiological temperatures and exhibits thermosensitivity at 37°C. Obviously, there are evolutionary constraints which cannot be completely overcome by the human TAP–p15 complex in yeast. Independently of this incomplete complementation, it is clear that TAP and p15 have to assemble into a complex in yeast to become functionally active. Since no complex formation could be measured *in vitro* between TAP and Mtr2p (J.Katahira, unpublished data), cross-species complexes such as TAP–Mtr2p or Mex67p–p15 may not form.

Strikingly, the TAP–p15 complex, once formed in yeast, can fulfill functions that are normally accomplished by the Mex67p–Mtr2p complex, such as binding to mRNPs, interaction with components of the nuclear pore complex and dissociation of the complex from distinct nucleoporins into the cytoplasm (e.g. from Nup159p which is the putative homologue of CAN/Nup214). TAP and Mex67p are structurally conserved during evolution which explains well the observed functional TAP-mediated complementation in yeast. In contrast, p15 and Mtr2p, although performing a similar function within their respective complexes, are at first sight structurally not homologous. However, it would not be surprising if both proteins have a similar overall folding.

In summary, we have characterized human TAP (TIP-associating protein) as a homologue of yeast Mex67p. Strikingly, the multi-domain protein TAP can directly associate with nucleoporins and poly(A)$^+$ RNA, and tightly binds to p15, a member of the NTF2 protein family (Figure 9). For functional complementation in yeast, TAP requires co-expression of p15. Thus, the TAP–p15 complex

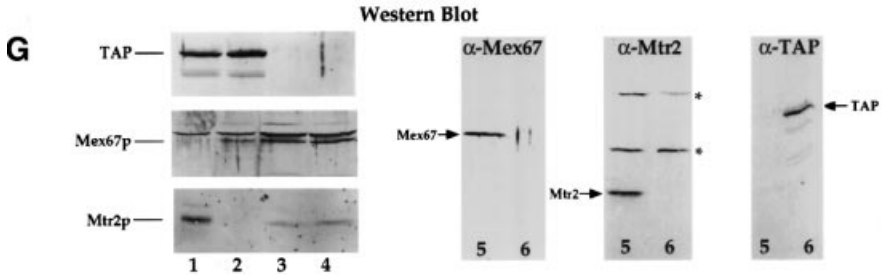

Fig. 8. The human TAP–p15 complex is functionally active in yeast. (A–C) Intracellular location of GFP–TAP in yeast. Wild-type (**A**), nup133$^-$ (**B**), and mtr2-13 (**C**) yeast cells expressing GFP–TAP were inspected in the fluorescence microscope. The insert in (A) shows a picture processed by digital confocal imaging ('deconvolution'; available as a module within the software program 'Openlab', Improvision, Coventry, UK). In mtr2-13 cells (C), GFP–TAP mislocalizes into cytoplasmic spots upon a 15 min shift to the restrictive temperature. (**D**) Intracellular location of GFP–p15 in yeast cells co-expressing human TAP. (**E**) Complementation of yeast mtr2$^-$ and mex67$^-$ strains by co-expression of human TAP and p15. Strains *mtr2::HIS3* null complemented by plasmid-borne pURA3-MTR2 and *mex67::HIS3* null complemented by pURA3-MEX67 were co-transformed with 2μ plasmids pLEU2-TAP and pADE2-p15 (TAP/P15), pLEU2 empty and pADE2-p15 (p15), pLEU2-TAP and pADE2 empty (TAP), pLEU2-MTR2 or pLEU2-MEX67 and pADE2 empty (MTR2 or MEX67) and pLEU2 empty and pADE2 empty (–). Two individual transformants were first grown on selective SDC –leu –ade plate, before plating on 5-FOA plates. On these plates, only cells which have lost the pURA3-MTR2 and pURA3-MEX67 plasmids, respectively, can grow. After 8 days incubation at 23°C, small colonies became visible, but only in the case of TAP–p15 co-expression. Plates were incubated for 15 days before pictures were taken. (**F**) Growth properties of mtr2$^-$ and mex67$^-$ single disruption strains and the mex67$^-$–mtr2$^-$ double knockout mutant complemented by the human TAP–p15 complex. The strains *mex67::HIS3* + pLEU2-TAP/pADE2-p15 (mex67$^-$ + TAP–p15), *mtr2::HIS3* + pLEU2-TAP/pADE2-p15 (mtr2$^-$ + TAP–p15), *mex67::HIS3* + pLEU2-MEX67 (mex67$^-$ + MEX67), *mtr2::HIS3* + pLEU2-MTR2 (mtr2$^-$ + MTR2) and *mex67::HIS3/mtr2::HIS3* + pLEU2-TAP/pADE2-p15 (mex67$^-$/mtr2$^-$ + TAP–p15) were constructed as described in the Materials and methods. Precultures were diluted in growth medium and equivalent amounts of cells (diluted in 10^{-1} steps) were spotted onto YPD plates. Plates were incubated for 6 days at the temperatures indicated. Two independent growth experiments are shown. (**G**) Expression of human TAP in yeast. Whole-cell lysates derived from strains (lane 1) *mex67::HIS3* + pLEU2-TAP/pADE2-p15, (2) *mtr2::HIS3* + pLEU2-TAP/pADE2-p15, (3) *mex67::HIS3* + pLEU2-MEX67, (4, 5) *mtr2::HIS3* + pLEU2-MTR2 and (6) *mex67::HIS3/mtr2::HIS3* + pLEU2-TAP/pADE2-p15 were analyzed by SDS–PAGE and Western blotting using antibodies against human TAP-C, yeast Mtr2p and Mex67p. In the left panel only the relevant area of the blot is shown and the crude immune sera were used. In the right panel, affinity-purified anti-Mex67p and anti-Mtr2p antibodies were used. The bands corresponding to TAP, Mex67p and Mtr2p are indicated. Note that the affinity-purified anti-Mtr2p antibody still cross-reacts with two higher mol. wt bands (indicated by asterisks).

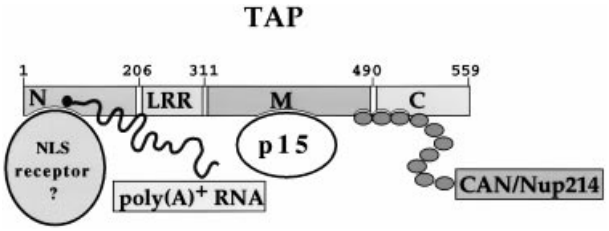

Fig. 9. A model of TAP organization and its interacting proteins.

is an evolutionarily conserved complex required for nuclear mRNA export.

Materials and methods

Yeast methods and DNA recombinant work

Yeast strains used in this study were described by Santos-Rosa *et al*. (1998) and grown and transformed according to Segref *et al*. (1997). Manipulation and analysis of DNA such as restriction analysis, end-filling, ligations, DNA sequencing and PCR amplifications were performed according to Maniatis *et al*. (1982). Microscopic observation of GFP fusion proteins in yeast was carried out as described by Segref *et al*. (1997).

Plasmid constructions

The *TAP* cDNA was excised from plasmid pJ3TAP (Yoon *et al*., 1997) and subcloned into pBluescript SK (Stratagene, Heidelberg, Germany). To generate a GFP-tagged TAP expression vector in yeast, *TAP* cDNA was subcloned into the pNOPGFP vector (Hellmuth *et al*., 1998). To generate vectors for expression of untagged TAP and p15 in yeast, 2μ high copy number plasmids (with either the *LEU2* or *ADE2* marker) were used. The cDNAs of *TAP* or *p15* were placed under the *NOP1* promoter and 3′ untranslated region (UTR) sequences from the *ADHI* terminator were attached at the 3′ end. To construct a full-length TAP–GFP expression vector for mammalian cells, *TAP* cDNA was introduced to the pCMX-SAH/Y145F vector (Ogawa and Umesono, 1998). N- and C-terminal TAP–GFP truncation mutants were constructed by using a convenient restriction site within *TAP*. For *E.coli* expression, *TAP* cDNA fragments encoding the N-domain (aa 1–154) and C-domain (aa 320–559) of TAP were amplified by PCR and subcloned into the pET8c-HIS6 vector as described previously (Santos-Rosa *et al*., 1998).

To construct the bait plasmid for the two-hybrid screen, full-length *TAP* was fused to the *GAL4* DNA-binding domain within the pAS2 vector. To construct prey plasmids for the series of CAN/Nup214 deletion mutants, corresponding DNA fragments were PCR-amplified and subcloned into the pACT2 prey vector. N- and C-terminal TAP deletion mutants were constructed using appropriate restriction sites or by PCR. To construct GST-tagged CAN3 and CAN4 expression vectors, CAN3 and CAN4 fragments were isolated from the two-hybrid prey plasmids and inserted into the pGEX4T-3 vector (Pharmacia, Freiburg, Germany). GST–CAN4, which was unstable in *E.coli*, was tagged at its C-terminus with His_6, which allowed better purification of this construct. Untagged, full-length TAP or deletion constructs, TAP-N (aa 1–300) and TAP-M (aa 294–499), were also inserted into pET-9d vector. The entire open reading frame (ORF) of human p15 cDNA present in the human testis library (see above) was amplified by nested PCR using appropriate 5′ *Xho*I and 3′ *Mlu*I primers. This PCR fragment was digested with *Xho*I and *Mlu*I and inserted into the pET8c vector. The PCR-derived p15 cDNA clone was sequenced and no mutations were found.

For expression of GFP–TAP and GFP–p15 in yeast RS453 cells, high copy number (2μ) plasmids containing GFP–TAP and GFP–p15, respectively, were constructed. The *TAP* gene was fused to GFP and the hybrid construct placed under the control of the *NOP1* promoter. The fusion gene was inserted into the 2μ plasmid pRS424 (TRP1), and the *ADHI* terminator sequence derived from pACTII was attached to the 3′-end of the *GFP–TAP* fusion gene. The resulting plasmid is designated pRS424-P_{NOP1}::GFP–TAP1::ADH1. GFP-tagged p15 was made by PCR amplification of the p15 ORF with the appropriate primers creating a *Hin*dIII site at the start codon and *Xho*I site after the stop codon. This PCR product was inserted into a pLEU2-P_{NOP1}-GFP vector (*GFP* under the control of the *NOP1* promoter) cut with *Hin*dIII–*Xho*I allowing in-frame fusion between GFP and p15.

Two-hybrid screens using TAP or MEX67 as bait

The yeast two-hybrid screening strain HF7c harboring the pAS2-TAP bait plasmid was transformed with a human testis cDNA library (Clontech). In total, 1.5×10^6 transformants were obtained, of which ~3000 colonies grew on SDC (–leu, –trp, –his) plates containing 3 mM 3-amino-1, 2, 4-triazole. These colonies were tested for β-galactosidase activity using the X-Gal filter assay. Prey plasmids were recovered from $HIS^+/lacZ^+$ colonies and this phenotype was confirmed by retransforming the HF7c strain harboring pAS2-TAP with the isolated prey plasmids. Finally, 32 clones, which fulfilled the requirement for specific interaction with TAP, were analyzed by DNA restriction and cDNA inserts were sequenced (TOPLAB, Munich, Germany). To analyze two-hybrid interactions between Mex67p as bait and FG repeat sequences from nucleoporins as preys, the two-hybrid assay was performed exactly as previously described, with the exception that the entire MEX67 ORF was inserted into the pAS2 plasmid (Segref *et al*., 1997). In the case of pACTII-NUP159, the FG-repeat domain of Nup159p corresponding to residues 460–752 was cloned by PCR amplification with the respective primers and inserted into pACTII cut with *Nco*I and *Xho*I.

Generation of TAP and p15 antibodies

Recombinant TAP-N produced in *E.coli* BL21 (plasmid pET-TAP-N) was soluble and purified on Ni-NTA columns (Qiagen, Hilden, Germany) followed by MonoS FPLC. The TAP-C domain was, however, found in inclusion bodies, which was solubilized with 20 mM Tris–HCl pH 8.0, 150 mM NaCl, 5 mM $MgCl_2$, 8 M urea and partially purified by Ni-NTA chromatography. Antibodies against purified TAP-N and TAP-C domains were raised in rabbits (Eurogentech, Ougree, Belgium). The anti-TAP-C serum was affinity-purified on nitrocellulose strips containing the TAP recombinant protein. Two-month-old rabbits were immunized with histidine-tagged and purified p15. Antibodies against p15 were affinity-purified by nitrocellulose membrane strips which contain purified histidine-tagged p15. Affinity-purified anti-p15 antibodies were used in a 1:20 dilution for indirect immunofluorescence.

Cell culture, transfection and yeast complementation

HeLa and NIH 3T3 cells were maintained in Dulbecco's modified Eagle's medium (DMEM; Gibco-BRL, Karlsruhe, Germany) supplemented with 10% fetal calf serum (FCS; Gibco-BRL) at 37°C under 5% CO_2 in air. A *Xenopus* kidney epithelial cell line A6 cells (a kind gift from Dr E.Karsenti, EMBL, Heidelberg, Germany) were cultured in Leibovitz F15 medium (Sigma, Munich, Germany) supplemented with 10% FCS and 30% distilled water (A6 medium) at 23°C in air. Transfection was performed using Superfect transfection reagent (Qiagen) according to the company's manual. Twenty-four to 48 h after transfection, cells were processed for further analysis.

For TAP–p15-mediated complementation of yeast single disruption mutants *mtr2::HIS3* and *mex67::HIS3* and the double disruption mutant *mtr2::HIS3/mex67::HIS3*, the genes encoding human TAP and p15 under the control of the *NOP1* promoter were inserted into 2μ high copy number plasmids yielding plasmids pLEU2-TAP and pADE2-p15. These plasmids were transformed into the MEX67 shuffle strain (mex67::HIS3 + pURA3-MEX67), MTR2 shuffle strain (mtr2::HIS3 + pURA3-MEX67) and MTR2/MEX67 shuffle strain (mtr2:HIS3/mex67::HIS3 + pURA3-MTR2 + pTPR1-mex67-5) (Santos-Rosa *et al*., 1998) and it was selected on SDC –leu –ade plates, before transfer on 5-fluoro-orotic acid (5-FOA) plates. On 5-FOA plates, only cells which have lost pURA3-MEX67 and pURA3-MTR2 plasmids, respectively, can grow. Only after prolonged incubation (>10 days) at 23°C, small colonies became visible in the case of TAP–p15 co-expression. The *mex67::HIS/mtr2::HIS3* double disruption mutant expressing already TAP–p15, but still containing mex67-5 on a *TRP1* plasmid (mtr2:HIS3/mex67::HIS3 + pTPR1-mex67-5 + pLEU2-TAP + pADE2-p15) was transformed with the pURA3-MEX67 plasmid and a transformant which lost the pTRP1-mex67-5 plasmid was further incubated on a 5-FOA containing plate, yielding strain mtr2::HIS/mex67::HIS3 + pLEU2-TAP + pADE2-p15.

Immunofluorescence and heterokaryon assay

Normal tissue culture cells or heterokaryon cells grown on coverslips were fixed with 4% paraformaldehyde for 15 min and permeabilized with 0.2% Triton X-100. In some cases, HeLa cells were extracted on coverslips with different reagents [CSK buffer: 100 mM NaCl, 300 mM sucrose, 10 mM PIPES pH 6.8, 3 mM $MgCl_2$, 0.5% Triton X-100, 1.2 mM PMSF; high salt buffer: 250 mM $(NH_4)_2SO4$, 300 mM sucrose, 10 mM PIPES pH 6.8, 3 mM $MgCl_2$, 1.2 mM PMSF, 0.5% Triton X-100; nuclease buffer: 50 mM NaCl, 300 mM sucrose, 10 mM PIPES pH 6.8, 3 mM $MgCl_2$, 0.5% Triton X-100, 1.2 mM PMSF, 100 μg/ml

of DNaseI and RNase] exactly as described by Carmo-Fonseca *et al*. (1991), before indirect immunofluorescence using affinity-purified anti-TAP and anti-p15 antibodies. After washing with phosphate-buffered saline (PBS), cells were incubated for 30 min with first antibodies (diluted in PBS, 2% BSA) which were polyclonal anti-TAP (see above), monoclonal anti-fibrillarin (Aris and Blobel, 1991), monoclonal anti-human hnRNP A and C, polyclonal anti-GST (Pharmacia, Freiburg, Germany) and monoclonal MAb 414 (anti-nucleoporin). After washing, secondary antibodies were used which were Cy3-labeled donkey anti-rabbit IgG (Jackson ImmunoResearch Laboratories, West Grove, CA) and FITC-labeled goat anti-mouse IgG (Catalog Laboratories, Burlingame, CA). After washing with PBS, the immunofluorescence signals were analyzed with a Zeiss Axiskop fluorescence microscope and pictures were taken with a Xillix Microimager CCD camera.

The heterokaryon assay was done essentially according to Pinol-Roma and Dreyfuss (1992). Briefly, HeLa or NIH 3T3 cells were harvested by trypsinization and co-cultured with A6 cells grown on cover slips in 24-well culture plates for 3 h at 30°C in A6 medium. After treatment with cycloheximide (100 μg/ml) for 30 min, the cells were washed with Leibovitz F15 medium supplemented with 30% distilled water and treated with 50% PEG 1500 for 2 min at room temperature. After washing, the cells were cultured in A6 medium at 30°C for 4 h in the presence of cycloheximide (100 μg/ml). The heterokaryons were then subjected to indirect immunofluorescence using anti-TAP-C and anti-hnRNP A1 or C1/C2 antibodies.

Immunoprecipitation of p15 and mass spectrometry

For small scale immunoprecipitation, subconfluent HeLa cell cultures (2×10^6 cells) were labeled for 8 h with 100 μCi/ml of [^{35}S]methionine/cystein and immunoprecipitated according to standard protocols (Katahira *et al*., 1997) with 10 μl of protein G–Sepharose beads, previously treated with pre-immune serum, or anti-TAP-N and anti-TAP-C antibodies. Immunoprecipitated proteins were eluted from the beads by boiling in SDS–PAGE sample buffer, and labeled bands were visualized by fluorography or Western blotting. For large scale immunoprecipitation, a HeLa cell nuclear extract derived from 5×10^9 cells (Computor Cell Culture Center, Mons, Belgium) was dialyzed against buffer [20 mM sodium phosphate, pH 7.4, 100 mM NaCl, 5 mM $MgCl_2$, 1 mM dithiothreitol (DTT), 10% glycerol, 0.05% Tween-20] and fractionated by MonoS FPLC chromatography. TAP-containing fractions, which were identified by Western blotting, eluted between 0.6 and 0.8 M NaCl and were dialyzed against PBS containing 5 mM $MgCl_2$, 1 mM DTT and 1% NP-40. The dialyzed fraction was pre-cleared with 25 μl of Sephadex G-25 beads, before it was incubated with 50 μl of protein A–Sepharose beads to which anti-TAP-C antibodies were covalently attached (Schneider *et al*., 1982). It was incubated for 4 h at 4°C before beads were washed twice with 10 ml of PBS, 5 mM $MgCl_2$, 1 mM DTT and 1% NP-40. The bound proteins were eluted in 0.4 ml of 1% SDS and precipitated by acetone. This final immune pellet was solubilized in 30 μl of SDS-sample buffer and loaded onto 14% SDS–polyacrylamide gel.

Immunoprecipitated TAP and p15 were identified using a two-stage mass spectrometry strategy described previously (Shevchenko *et al*., 1996a), with minor modifications. Briefly, the protein bands were excised from polyacrylamide gels, washed, reduced, alkylated and in-gel digested with an excess of trypsin (Shevchenko *et al*., 1996b). For peptide mass fingerprinting, 1–3% of of recovered peptide mixture was analyzed on a Bruker REFLEX time-of-flight mass spectrometer (Bruker-Daltonics, Bremen, Germany) as described previously (Jensen *et al*., 1996). For peptide sequencing, half of the remaining peptide mixture was taken directly from the supernatant and loaded onto a small volume (70 nl) of POROS R2 (Perseptive, Framingham, MA) beads suspended in a capillary. After desalting, the concentrated peptide mixture was eluted into a nanoelectrospray needle (Protana, Odense, Denmark; Wilm and Mann, 1996; Wilm *et al*., 1996). Peptides were sequenced on a prototype quadrupole time-of-flight instrument (QqTOF, PE-SCIEX, Toronto, Canada). For the analysis of unknown proteins, the digestion was performed in 70:30 ^{16}O:^{18}O water as described previously (Shevchenko *et al*., 1997). Peptide Search software was used for database searching both with nrdb and ESTs databases (Mann and Wilm, 1994). Multiple sequence alignment was done using 'ClustalW1.6' (BCM Search Launcher) and 'Boxshade' (http://ulrec3.unil.ch/software/BOX_form.html).

UV-crosslinking of TAP to poly(A)$^+$ RNAs and band-shift assay

Isolation of UV-crosslinked RNA–protein complex from HeLa cells and analysis of crosslinked proteins by Western blotting were done as described by Pinol-Roma *et al*. (1989a). Exponentially growing HeLa cells (2×10^7) were washed in PBS and UV-crosslinked in a Stratalinker (Stratagene). Total cell extracts from the crosslinked or non-crosslinked cells were purified twice on oligo(dT) cellulose columns (Pharmacia, Freiburg, Germany). After the second elution, poly(A)$^+$ RNA-containing fractions were pooled, ethanol precipitated and digested with RNase A (100 μg/ml; Sigma). Whole-cell lysates and RNase A-treated eluates were analyzed by SDS–PAGE and Western blotting. RNA band-shift assays using recombinant TAP were performed as described previously (Santos-Rosa *et al*., 1998), except that 0.5% Tween-20 was included in binding buffer, and binding reactions and electrophoresis were carried out at 4°C.

Purification of the TAP–p15 complex and p15 from E.coli

Expression of p15 and TAP in *E.coli* was done according to Santos-Rosa *et al*. (1998). *Escherichia coli* BL21 cells harboring pET9d-TAP (untagged TAP) together with (i) pET8c empty vector, (ii) pET8c-p15, (iii) pET8c-Arc1p and (iv) pET8c-yNTF2p, respectively, were induced by 0.2 mM isopropyl-β-D-galactopyranoside (IPTG). Soluble cell lysate (6 ml) in 20 mM Tris–HCl, pH 8.0, 50 mM NaCl, 5 mM $MgCl_2$, 20 mM imidazole, 10% glycerol, 0.5% Tween-20 was mixed with 80 μl of Ni-NTA beads. It was washed twice with 10 ml of lysis buffer and once with 3 ml lysis buffer containing 0.5 M NaCl. Bound proteins were eluted with the lysis buffer containing 200 mM imidazole and analyzed by SDS–PAGE and Western blotting.

Solution binding assay

GST alone, or GST-tagged CAN3 and CAN4 were immobilized on glutathione–Sepharose beads. After washing with universal buffer (Kunzler and Hurt, 1998), histidine-tagged TAP (~2 μg) in 200 μl buffer were applied. After incubating at 4°C for 1 h, columns were washed and the bound proteins were eluted by SDS-sample buffer. Bound (25% of the total eluate) and unbound fractions (7.4% as compared with the load) were analyzed by SDS–PAGE and Coomassie/silver staining, or Western blotting using the anti-TAP-C antibody.

Recombinant and purified p15 and yeast NTF2 were also covalently attached to NHS–Sepharose beads (100 μl), using the same amounts of proteins in the coupling reaction (100 μg) according to Clarkson *et al*. (1996). The coupling efficiency was calculated by comparing the protein concentration of p15 and yNTF2 containing solutions before and after coupling reaction. The coupling efficiency was >80%, in both cases.

SDS–PAGE and Western blotting

Whole-cell extracts were prepared from *mex67::HIS3* and *mtr2::HIS3* single-disrupted, and *mex67::HIS3/mtr2::HIS3* double-disrupted strains, complemented by either *MEX67* and *MTR2*, or the TAP–p15 complex. For lysis of the cells, the glass bead method was used and it was extracted with hot SDS-sample buffer. An equivalent amount of cells corresponding to 1 OD_{600} were analyzed by SDS–PAGE and Western blotting using the anti-TAP-C, anti-Mex67p and anti-Mtr2p antibodies as described previously (Santos-Rosa *et al*., 1998).

Acknowledgements

We thank Alexandra Segref for excellent technical assistance in the initial phase of this project. We are grateful to Dr K.Umesono (Kyoto University, Japan) for providing vector pCMX-SAH/Y145F and Dr R.Bischoff (DKFZ, Heidelberg, Germany) for recombinant Ran. Monoclonal antibodies against human hnRNP A1 and hnRNP C were generous gifts from Dr G.Dreyfuss (Howard Hughes Medical Institute, University of Pennsylvania, Philadelphia, PA). We are also grateful to members of our laboratory, especially Drs G.Simos and M.Kunzler for critical reading of the manuscript. E.C.H. is the recipient of a grant from the Deutsche Forschungsgemeinschaft (SFB352) and J.K. is a holder of an Alexander von Humboldt fellowship.

References

Aris,J.P. and Blobel,G. (1991) cDNA cloning and sequencing of human fibrillarin, a conserved nucleolar protein recognized by autoimmune antisera. *Proc. Natl Acad. Sci. USA*, **88**, 931–935.

Arts,G.-J., Fornerod,M. and Mattaj,I.W. (1998) Identification of a nuclear export receptor for tRNA. *Curr. Biol.*, **8**, 305–314.

Bastos,R., Lin,A., Enarson,M. and Burke,B. (1996) Targeting and function in mRNA export of nuclear pore complex protein Nup153. *J. Cell Biol.*, **134**, 1141–1156.

Belgareh,N., Snay-Hodge,S., Pasteau,F., Dahger,S., Cole,C. and Doye,V. (1998) Functional characterization of a Nup159p-containing nuclear pore subcomplex. *Mol. Biol. Cell*, **9**, 3475–3492.

Boer,J.M., Van Deursen,J.M.A., Croes,H.J., Fransen,J.A.M. and Grosveld,G.C. (1997) The nucleoporin CAN/Nup214 binds to both the cytoplasmic and the nucleoplasmic sides of the nuclear pore complex in overexpressing cells. *Exp. Cell Res.*, **232**, 182–185.

Bogerd,H.P., Fridell,R.A., Madore,S. and Cullen,B.R. (1995) Identification of a novel cellular cofactor for the Rev/Rex class of retroviral regulatory proteins. *Cell*, **82**, 485–494.

Borer,R.A., Lehner,C.F., Eppenberger,H.M. and Nigg,E.A. (1989) Major nucleolar proteins shuttle between nucleus and cytoplasm. *Cell*, **56**, 379–390.

Bullock,T.L., Clarkson,W.D., Kent,H.M. and Stewart,M. (1996) The 1.6 Å resolution crystal structure of nuclear transport factor 2 (NTF2). *J. Mol. Biol.*, **260**, 422–431.

Carmo-Fonseca,M., Kern,H. and Hurt,E.C. (1991) Human nucleoporin p62 and the essential yeast nuclear pore protein NSP1 show sequence homology and a similar domain organization. *Eur. J. Cell Biol.*, **55**, 17–30.

Clarkson,W., Kent,H. and Stewart,M.J. (1996) Separate binding sites on nuclear transport factor 2 (NTF2) for GDP-Ran and the phenylalanine-rich repeat regions of nucleoporins p62 and Nsp1p. *J. Mol. Biol.*, **263**, 517–524.

Conti,E., Uy,M., Leighton,L., Blobel,G. and Kuriyan,J. (1998) Crystallographic analysis of the recognition of a nuclear localization signal by the nuclear import factor karyopherin α. *Cell*, **94**, 193–204.

Dahlberg,J.E. and Lund,E. (1998) Functions of the GTPase ran in RNA export from the nucleus. *Curr. Opin. Cell Biol.*, **10**, 400–408.

Del priore,V., Heath,C.V., Snay,C.A., MacMillan,A., Gorsch,L.C., Dagher,S. and Cole,C.N. (1997) A structure/function analysis of Rat7p/Nup159p, an essential nucleoporin of *Saccharomyces cerevisiae*. *J. Cell Sci.*, **110**, 2987–2999.

Doye,V., Wepf,R. and Hurt,E.C. (1994) A novel nuclear pore protein Nup133p with distinct roles in poly(A)$^+$ RNA transport and nuclear pore distribution. *EMBO J.*, **13**, 6062–6075.

Dreyfuss,G., Matunis,M.J., Pinol-Roma,S. and Burd,C.G. (1993) hnRNP proteins and the biogenesis of mRNA. *Annu. Rev. Biochem.*, **62**, 289–321.

Fabre,E. and Hurt,E. (1997) Yeast genetics to dissect the nuclear pore complex and nucleocytoplasmic trafficking. *Annu. Rev. Genet.*, **31**, 277–313.

Fischer,U., Huber,J., Boelens,W.C., Mattaj,I.W. and Luhrmann,R. (1995) The HIV-1 Rev activation domain is a nuclear export signal that accesses an export pathway used by specific cellular RNAs. *Cell*, **82**, 475–483.

Fornerod,M., Ohno,M., Yoshida,M. and Mattaj,I.W. (1997a) CRM1 is an export receptor for leucine-rich nuclear export signals. *Cell*, **90**, 1051–1060.

Fornerod,M., Vandeursen,J., Vanbaal,S., Reynolds,A., Davis,D., Gopal Murti,K., Fransen,J. and Grosveld,G. (1997b) The human homologue of Yeast Crm1 is in a dynamic subcomplex with Can/Nup214 and a novel nuclear pore component Nup88. *EMBO J.*, **16**, 807–816.

Fukuda,M., Asano,S., Nakamura,T., Adachi,M., Yoshida,M., Yanagida,M. and Nishida,E. (1997) CRM1 is responsible for intracellular transport mediated by the nuclear export signal. *Nature*, **390**, 308–311.

Gabler,S., Schutt,H., Groitl,P., Wolf,H., Shenk,T. and Dobner,T. (1998) E1B 55-kilodalton-associated protein: a cellular protein with RNA-binding activity implicated in nucleocytoplasmic transport of adenovirus and cellular mRNAs. *J. Virol.*, **72**, 7960–7971.

Gorlich,D. (1998) Transport into and out of the cell nucleus. *EMBO J.*, **17**, 2721–2727.

Gruter,P., Tabernero,C., von Kobbe,C., Schmitt,C., Saavedra,C., Bachi,A., Wilm,M., Felber,B.K. and Izaurralde,E. (1998) TAP, the human homolog of Mex67p, mediates CTE-dependent RNA export from the nucleus. *Mol. Cell*, **1**, 649–659.

Hellmuth,K., Lau,D.M., Bischoff,F.R., Kunzler,M., Hurt,E.C. and Simos,G. (1998) Yeast Los1p has properties of an exportin-like nucleocytoplasmic transport factor for tRNA. *Mol. Cell. Biol.*, **18**, 6364–6386.

Huber,J., Cronshagen,U., Kadokura,M., Marshallsay,C., Wada,T., Sekine,M. and Luhrmann,R. (1998) Snurportin1, an m_3G-cap-specific nuclear import receptor with a novel domain structure. *EMBO J.*, **17**, 4114–4126.

Hurwitz,M.E., Strambio-de-Castillia,C. and Blobel,G. (1998) Two yeast nuclear pore complex proteins involved in mRNA export form a cytoplasmically oriented subcomplex. *Proc. Natl Acad. Sci. USA*, **95**, 11241–11245.

Jensen,O.N., Podtelejnikov,A. and Mann,M. (1996) Delayed extraction improves specificity in database searches by matrix-assisted laser desorption/ionization peptide maps. *Rapid Commun. Mass Spectrom.*, **19**, 1371–1378.

Katahira,J., Inoue,N., Horiguchi,Y., Matsuda,M. and Sugimoto,N. (1997) Molecular cloning and functional characterization of the receptor for *Clostridium perfringens* enterotoxin. *J. Cell Biol.*, **136**, 1239–1247.

Kraemer,D., Wozniak,R.W., Blobel,G. and Radu,A. (1994) The human CAN protein, a putative oncogene product associated with myeloid leukemogenesis, is a nuclear pore complex protein that faces the cytoplasm. *Proc. Natl Acad. Sci. USA*, **91**, 1519–1523.

Kraemer,D.M., Strambio-de-Castillia,C., Blobel,G. and Rout,M.P. (1995) The essential yeast nucleoporin NUP159 is located on the cytoplasmic side of the nuclear pore complex and serves in karyopherin-mediated binding of transport substrate. *J. Biol. Chem.*, **270**, 19017–19021.

Kunzler,M. and Hurt,E.C. (1998) Cse1p functions as the nuclear export receptor for importin α in yeast. *FEBS Lett.*, **433**, 185–190.

Kutay,U., Bischoff,F.R., Kostka,S., Kraft,R. and Gorlich,D. (1997) Export of importin α from the nucleus is mediated by a specific nuclear transport factor. *Cell*, **90**, 1061–1071.

Kutay,U., Lipowsky,G., Izaurralde,E., Bischoff,F.R., Schwarzmaier,P., Hartmann,E. and Gorlich,D. (1998) Identification of a tRNA-specific nuclear export receptor. *Mol. Cell*, **1**, 359–369.

Maniatis,T., Fritsch,E.T. and Sambrook,J. (1982) *Molecular Cloning: A Laboratory Manual*. Cold Spring Harbor Laboratory Press, Cold Spring Harbor, New York.

Mann,M. and Wilm,M.S. (1994) Error tolerant identification of peptides in sequence databases by peptide sequence tags. *Anal. Chem.*, **66**, 4390–4399.

Mattaj,I.W. and Englmeier,L. (1998) Nucleocytoplasmic transport: The soluble phase. *Annu. Rev. Biochem.*, **67**, 265–306.

Matunis,E.L., Matunis,M.J. and Dreyfuss,G. (1992) Characterization of the major hnRNP proteins from *Drosophila melanogaster*. *J. Cell Biol.*, **116**, 257–269.

Matunis,M.J., Matunis,E.L. and Dreyfuss,G. (1993) PUB1: A major yeast poly(A)$^+$ RNA-binding protein. *Mol. Cell. Biol.*, **13**, 6114–6123.

Michael,W.M., Choi,M.Y. and Dreyfuss,G. (1995) A nuclear export signal in hnRNP A1: A signal-mediated, temperature-dependent nuclear protein export pathway. *Cell*, **83**, 415–422.

Nakielny,S. and Dreyfuss,G. (1996) The hnRNP C proteins contain a nuclear retention sequence that can override nuclear export signals. *J. Cell Biol.*, **134**, 1365–1373.

Nakielny,S. and Dreyfuss,G. (1997) Import and export of the nuclear protein import receptor transportin by a mechanism independent of GTP hydrolysis. *Curr. Biol.*, **8**, 89–95.

Neville,M., Stutz,F., Lee,L., Davis,L.I. and Rosbash,M. (1997) The importin-β family member Crm1p bridges the interaction between Rev and the nuclear pore complex during nuclear export. *Curr. Biol.*, **7**, 767–775.

Ogawa,H. and Umesono,K. (1998) Intracellular localization and transcriptional activation by the human glucocorticoid receptor–green fluorescent protein (GFP) fusion proteins. *Acta Histochem. Cytochem.*, **31**, 303–308.

Ohno,M., Fornerod,M. and Mattaj,I.W. (1998) Nucleocytoplasmic transport: The last 200 nanometers. *Cell*, **92**, 327–336.

Ossareh-Nazari,B., Bachelerie,F. and Dargemont,C. (1997) Evidence for a role of CRM1 in signal-mediated nuclear protein export. *Science*, **278**, 141–144.

Percipalle,P., Clarkson,W.D., Kent,H.M., Rhodes,D. and Stewart,M. (1997) Molecular interactions between the importin α/β heterodimer and proteins involved in vertebrate nuclear protein import. *J. Mol. Biol.*, **266**, 722–732.

Pinol-Roma,S. and Dreyfuss,G. (1992) Shuttling of pre-mRNA binding proteins between nucleus and cytoplasm. *Nature*, **355**, 730–732.

Pinol-Roma,S., Adam,S.A., Choi,Y.D. and Dreyfuss,G. (1989a) Ultraviolet-induced cross-linking of RNA to proteins *in vivo*. *Methods Enzymol.*, **180**, 410–418.

Pinol-Roma,S., Swanson,M.S., Gall,J.G. and Dreyfuss,G. (1989b) A novel heterogenous nuclear RNP protein with a unique distribution on nascent transcripts. *J. Cell Biol.*, **109**, 2575–2587.

Powers,M.A., Forbes,D.J., Dahlberg,J.E. and Lund,E. (1997) The vertebrate GLFG nucleoporin, Nup98, is an essential component of multiple RNA export pathways. *J. Cell Biol.*, **136**, 241–250.

Reichelt,R., Holzenburg,E.L., Buhle,E.L., Jarnik,M., Engel,A. and Aebi,U. (1990) Correlation between structure and mass distribution of nuclear pore complex components. *J. Cell Biol.*, **110**, 883–894.

Rexach,M. and Blobel,G. (1995) Protein import into nuclei: Association and dissociation reactions involving transport substrate, transport factors and nucleoporins. *Cell*, **83**, 683–692.

Ribbeck,K., Lipowsky,G., Kent,H.M., Stewart,M. and Gorlich,D. (1998) NTF2 mediates nuclear import of Ran. *EMBO J.*, **17**, 6587–6598.

Santos-Rosa,H., Moreno,H., Simos,G., Segref,A., Fahrenkrog,B., Pante,N. and Hurt,E. (1998) Nuclear mRNA export requires complex formation between Mex67p and Mtr2p at the nuclear pores. *Mol. Cell. Biol.*, **18**, 6826–6838.

Schneider,C., Newman,R.A., Sutherland,D.R., Asser,U. and Greaves, M.F. (1982) A one-step purification of membrane proteins using a high efficiency immunomatrix. *J. Biol. Chem.*, **257**, 10766–10769.

Segref,A., Sharma,K., Doye,V., Hellwig,A., Huber,J. and Hurt,E.C. (1997) Mex67p which is an essential factor for nuclear mRNA export binds to both poly(A)$^+$ RNA and nuclear pores. *EMBO J.*, **16**, 3256–3271.

Shevchenko,A. *et al.* (1996a) Linking genome and proteome by mass spectrometry: large-scale identification of yeast proteins from two dimensional gels. *Proc. Natl Acad. Sci. USA*, **93**, 14440–14445.

Shevchenko,A., Wilm,M., Vorm,O. and Mann,M. (1996b) Mass spectrometric sequencing of proteins from silver stained gels. *Anal. Chem.*, **68**, 850–858.

Shevchenko,A., Chernushevich,I., Ens,W., Standing,K.G., Thomson,B., Wilm,M. and Mann,M. (1997) Rapid 'de novo' peptide sequencing by a combination of nanoelectrospray, isotopic labeling and a quadrupole/time-of-flight mass spectrometer. *Rapid Commun. Mass Spectrom.*, **11**, 1015–1024.

Siniossoglou,S., Wimmer,C., Rieger,M., Doye,V., Tekotte,H., Weise,C., Emig,S., Segref,A. and Hurt,E.C. (1996) A novel complex of nucleoporins, which includes Sec13p and a Sec13p homolog, is essential for normal nuclear pores. *Cell*, **84**, 265–275.

Solsbacher,J., Maurer,P., Bischoff,F.R. and Schlenstedt,G. (1998) Cse1p is involved in export of yeast importin α from the nucleus. *Mol. Cell. Biol.*, **18**, 6805–6815.

Stade,K., Ford,C.S., Guthrie,C. and Weis,K. (1997) Exportin 1 (Crm1p) is an essential nuclear export factor. *Cell*, **90**, 1041–1050.

Stewart,M., Kent,H.M. and McCoy,A.J. (1998) Structural basis for molecular recognization between nuclear transport factor 2 (NTF2) and the GDP-bound form of Ras-family GTPase Ran. *J. Mol. Biol.*, **277**, 635–646.

Stutz,F. and Rosbash,M. (1998) Nuclear RNA export. *Genes Dev.*, **12**, 3303–3319.

Stutz,F., Neville,M. and Rosbash,M. (1995) Identification of a novel nuclear pore-associated protein as a functional target of the HIV-1 Rev protein in yeast. *Cell*, **82**, 495–506.

Ullman,K.S., Powers,M.A. and Forbes,D.J. (1997) Nuclear export receptors: From importin to exportin. *Cell*, **90**, 967–970.

Van Deursen,J., Boer,J., Kasper,L. and Grosveld,G. (1996) G_2 arrest and impaired nucleocytoplasmic transport in mouse embryos lacking the proto-oncogene *CAN/Nup214*. *EMBO J.*, **15**, 5574–5583.

Wente,S.R., Rout,M.P. and Blobel,G. (1992) A new family of yeast nuclear pore complex proteins. *J. Cell Biol.*, **119**, 705–723.

Wilm,M. and Mann,M. (1996) Analytical properties of the nano electrospray ion source. *Anal. Chem.*, **66**, 1–8.

Wilm,M., Shevchenko,A., Houthaeve,T., Breit,S., Schweigerer,L., Fotsis,T. and Mann,M. (1996) Femtomole sequencing of proteins from polyacrylamide gels by nano electrospray mass spectrometry. *Nature*, **379**, 466–469.

Yang,Q., Rout,M.P. and Akey,Ch.W. (1998) Three-dimensional architecture of the isolated yeast nuclear pore complex: functional and evolutionary implications. *Mol. Cell*, **1**, 223–234.

Yoon,D.-K., Lee,H., Seol,W., DeMaria,M., Rosenzweig,M. and Jung,J.U. (1997) Tap: a novel cellular protein that interacts with Tip of Herpesvirus saimiri and induces lymphocyte aggregation. *Immunity*, **6**, 571–582.

Received December 22, 1998; revised and accepted March 15, 1999